

jpl

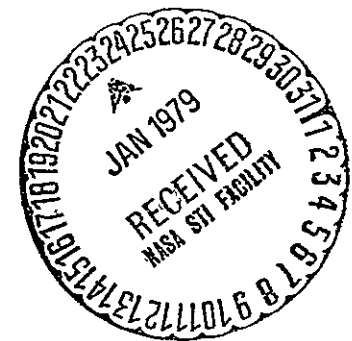
(NASA-CR-158041) APPLICABILITY OF THE  
REMOTE MOBILE EMPLACEMENT PACKAGE (RMEP)  
DESIGN AS A MOBILITY AID FOR PROPOSED  
POST-84 MARS MISSIONS, PHASE 0 (Grumman  
Aerospace Corp.) 78 p HC A05/MF A01

N79-14139

Unclas

G3/14

41956



JET PROPULSION LABORATORY  
CALIFORNIA INSTITUTE OF TECHNOLOGY  
PASADENA, CALIFORNIA

APPLICABILITY OF THE REMOTE MOBILE EMPLACEMENT PACKAGE (RMEP)  
DESIGN AS A MOBILITY AID FOR PROPOSED POST-84 MARS  
MISSIONS "PHASE O"

GAC Report #PDR-703-2

17 MAY 1978

JPL CONTRACT NO. 955064

THIS WORK WAS PERFORMED FOR THE JET PROPULSION  
LABORATORY, CALIFORNIA INSTITUTE OF TECHNOLOGY  
SPONSORED BY THE NATIONAL AERONAUTICS AND SPACE  
ADMINISTRATION UNDER CONTRACT NO. NAS7-100

GRUMMAN AEROSPACE CORPORATION  
BETHPAGE, NEW YORK 11714

## CONTENTS

Section	Page
ABSTRACT .....	1
1 <u>INTRODUCTION</u> .....	2
2 <u>VEHICLE CONFIGURATION</u> .....	4
2.1 Configuration Development .....	4
2.2 Mobility Characteristics of Point Designs .....	7
2.3 Reversing Travel .....	10
2.4 Remote Command .....	13
3 <u>CONFIGURATION DETAILS</u> .....	17
3.1 Wheels .....	17
3.2 Tail Extension .....	22
3.3 Flip-Over System .....	25
3.4 Tether Payout Device .....	25
3.5 Hazard Detection & Avoidance System (HDA) .....	27
3.5.1 Mechanical Hazard Sensor .....	30
3.5.2 Optical Techniques .....	31
4 <u>MOBILITY &amp; CONTROL SUBSYSTEM</u> .....	33
4.1 Control Configuration .....	35
4.2 Deployment & Erection .....	37
5 <u>MARS ENVIRONMENTAL EFFECT ON THE RMEP ELECTRICAL SYSTEM</u> .....	42
5.1 Mars Wind .....	42
5.2 Ground Slope & Obstacles .....	43
5.3 Ultraviolet Radiation .....	43
5.4 Temperature .....	43
5.5 Wheel Inflation Process .....	47
5.6 Rolling Resistance .....	50
5.7 Outgassing .....	50
5.8 Hard Landing (100-kg Vehicle) .....	50

CONTENTS (Contd)

<u>Section</u>		<u>Page</u>
6	<u>MMR RELIABILITY/SURVIVABILITY-GENERAL OBSERVATIONS</u> .....	52
7	<u>CONCLUSIONS &amp; RECOMMENDATIONS</u> .....	58
8	<u>ESTIMATED COST TO CONTINUE DEVELOPMENT OF THE RMEP</u> .....	59
<hr/>		
9	<u>NEW TECHNOLOGY</u> .....	59
	REFERENCES .....	60
	APPENDIX .....	61
	SURFACE HAZARD DETECTION .....	61

## ILLUSTRATIONS

<u>Fig.</u>	Title	<u>Page</u>
1	Basic Configurations Studied as Candidates for Remote Mobile Emplacement Systems . . . . .	3
2	Grumman's Remote Controlled Tactical Vehicle (RCTV) . . . . .	
3	General Arrangement MMR . . . . .	8
4	Approximation of Vehicle Total Locomotion Resistance vs Mass . . . . .	9
5	RMEP Wheel Drive System . . . . .	12
6	Suggested Sequence for Reverse Travel . . . . .	14
7	Interior Mechanical Arrangement - Front View . . . . .	15
8	Interior Mechanical Arrangement - Rear View . . . . .	16
9	Inflatable Toroidal Wheel Configuration . . . . .	18
10	Relative Work Required for Wheel Inflation at Different Pressures . . . . .	20
11	Relative Work Required for Wheel Inflation for Different Wheel Sizes . . . . .	21
12	Relative Work Required for Wheel Inflation for Different Tread Sizes . . . . .	23
13	Relative Work as a Function of Wheel Diameter . . . . .	24
14	Possible Boom Flip-Over Mechanism using Wheel Drive Motor . . . . .	26
15	Possible Umbilical Payout Concept . . . . .	28
16	Hazard Detection & Avoidance Subsystem Functional Block Diagram . . . . .	29
17	Mechanical Bumper . . . . .	31
18	Remote Mobile Emplacement Package - Stowed . . . . .	38
19	Erection & Deployment Time Sequence . . . . .	39
20	Sequence of Emplacement Operation . . . . .	40
21	Camera Mast Fully Extended . . . . .	41
22	Phase Diagram for CO <sub>2</sub> and H <sub>2</sub> O . . . . .	48
23	MARS Mini Rover Class I Mission . . . . .	53

## ILLUSTRATIONS (Contd)

<u>Fig.</u>	Title	<u>Page</u>
24	MARS Mini Rover Class II Mission . . . . .	53
25	Laser Cane Hazard Detection Technique . . . . .	64
26	Laser Cane Hole Detection . . . . .	66
27	Laser Cane Geometry for Slow Mode . . . . .	69
28	Azimuthal Field Coverage . . . . .	71
29	Laser Cane Simplified Block Diagram . . . . .	72

## TABLES

<u>Table</u>	Title	<u>Page</u>
1	Vehicle Classes . . . . .	5
2	Obstacle Clearance Requirements . . . . .	5
3	Total Locomotion Resistance on MARS . . . . .	11
4	Remote Command Capability . . . . .	13
5	RMEP Drive Motor-Gearbox . . . . .	34
6	RMEP Wheel Drive Growth Potential . . . . .	36
7	Thermal Requirements of Components . . . . .	46
8	RMEP/MMR Relative Mobility Data . . . . .	55

## ABSTRACT

This document is the result of a study to determine the applicability of the Grumman Remote Mobile Emplacement Package (RMEP) design concept as a mobility aid for the proposed post- '84 Mars Missions.

Three vehicles were identified by JPL:

- (a) A 20-kg, soft-landed mobility aid for tethered operation in support of a large lander vehicle
- (b) A similar, 50-kg vehicle
- (c) A 100-kg, hard-landed mobility aid, untethered, and communicating with an orbiter.

The RMEP wheel and mobility subsystem parameters: wheel tire size, weight, stowed volume, and environmental effects; obstacle negotiation; reliability and wear; motor and drive train; and electrical power demand were reviewed. Results indicated that: (1) the basic RMEP wheel design would be satisfactory, with additional attention to heating, side loading, tread wear and ultraviolet radiation protection; (2) motor and drive train power requirements on Mars would be less than on earth; and (3) the mobility electrical power requirements will be small enough to offer the option of operating the Mars Mini Rover untethered. Payload power required for certain sampling functions will preclude the use of battery power for these missions. Hazard avoidance and reverse direction maneuvers are discussed.

Limited examination of vehicle payload integration and thermal design was made, pending establishment of a baseline vehicle/payload design. No severely penalizing problems are anticipated, based on this analysis.

## Section 1

### INTRODUCTION

The principal objective of this study is to assess the applicability of the Remote Mobile Emplacement Package (RMEP) concept to the Mars Mini Rover (MMR) mission. The original RMEP, designed for terrestrial operation, had a mass of 9.07 kg and emphasized a high mobility to stowed volume ratio. Various configurations were studied for RMEP, Figure 1, and the tradeoffs, which apply as well to the MMR mission, showed that the vehicle with two large inflatable wheels best satisfied the requirements.

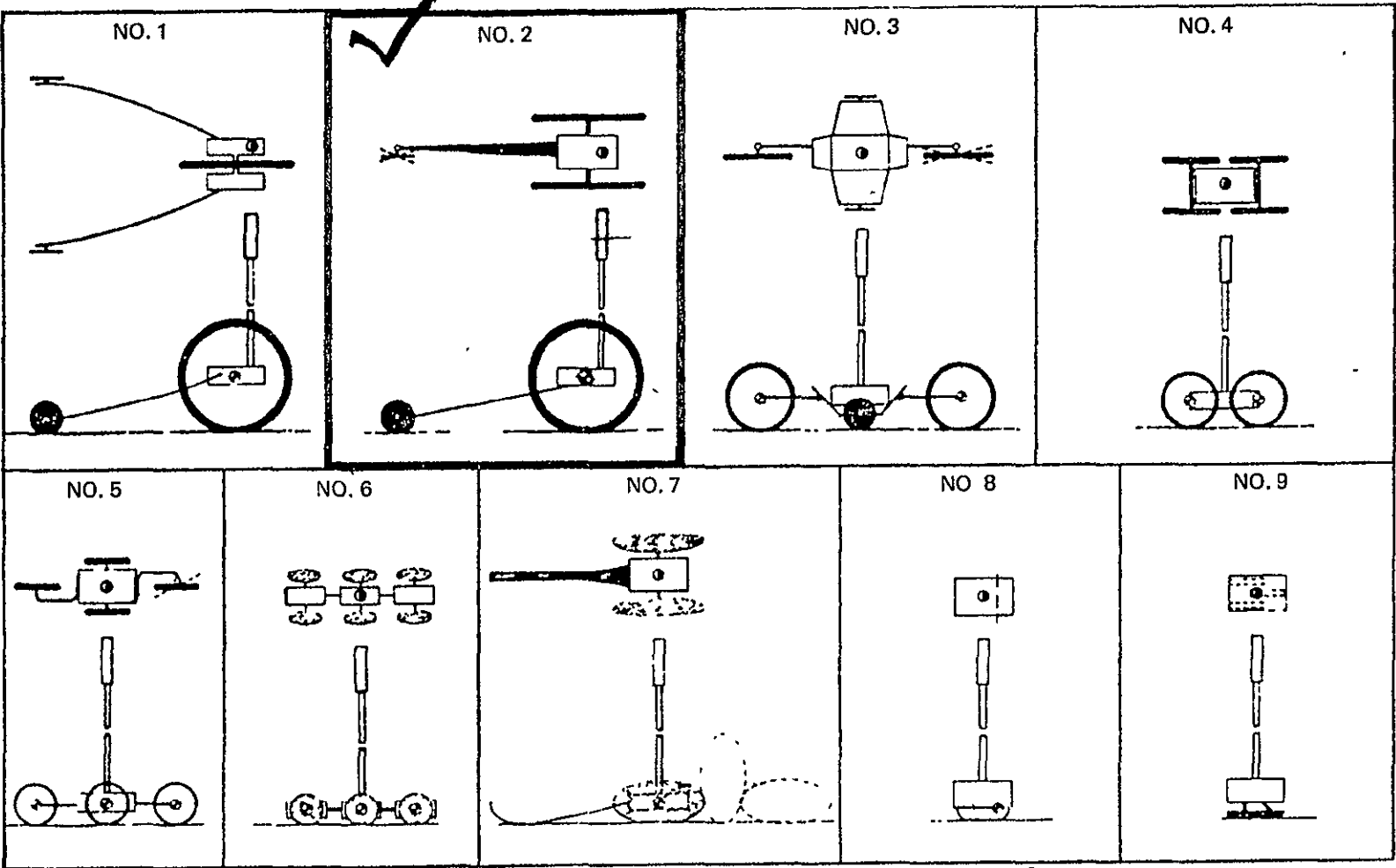


Fig. 1 Basic Configurations Studied as Candidates for Remote Mobile Emplacement Systems

## Section 2

### VEHICLE CONFIGURATION

MMR packaging requirements are less stringent than those of the RMEP, which had to stow in a volume of 10x6x4.8 inches before deployment. However, high packaging density is still vital for the MMR and the inflatable wheel approach provides the best ratio of deployed to stowed volume. Taking advantage of the slightly larger available packing volume, vehicle reliability can be improved by increasing tread thickness, overcoating the entire wheel, and decreasing the severity of folds.

Inflatable wheels offer two powerful advantages for MMR: first, they allow a much larger wheel to be carried in a small package, which lifts the payload high above obstructions when underway; and second, they offer a simple means to lower the payload repeatedly and provide high static stability and vibration resistance for experiment operations. Mechanically expanded "umbrella" type wheels could conceivably be made as large, but they would be complex and probably not collapsible, thus forfeiting the payload lowering feature.

It is of primary importance, therefore, to examine the inflatable wheels to reveal potential drawbacks and develop an acceptable response to each. Mechanical aspects of the pneumatic system appear to be straightforward and pumping energy requirements can be easily satisfied (see Paragraph 3.1.1). The most significant concern is maintaining the inflated shape while also resisting puncture and wear over a mission's duration. Thus, the central problem becomes one of wheel material and the detail design of the wheel "tire" and "skin". These are discussed in Subsection 3.1.

#### 2.1 CONFIGURATION DEVELOPMENT

Three vehicles and their missions were considered, as specified in JPL memos and summarized in Table 1. In addition to obstacle sizes and slopes, soil characteristics were assigned to estimate external resistance. The soil characteristics were taken from Reference A, published in 1974, except in the case of  $k_g$ , for which Reference B of 1977 provided an update. The obstacle clearance requirements listed in Table 2 dictate wheel diameters of at least 30 and 40 inches for Class a, b and c vehicles, respectively.

**TABLE 1 VEHICLE CLASSES**

VEHICLE CLASS	TOTAL WEIGHT		POWER & COMMUNICATIONS	RANGE (METERS)	
	(KG)	(LB)		DAILY	TOTAL
a SOFT LANDER	20	44	TETHERED &/OR UNTETHERED	1-3	200
b SOFT LANDER	50	110	TETHERED &/OR UNTETHERED	1-3	200
c HARD LANDER	100	220	UNTETHERED	1-3	2000

**TABLE 2 OBSTACLE CLEARANCE REQUIREMENTS**

CLASS	OBSTACLE
a	30 cm (11.8 IN.)
b	30 cm (11.8 in )
c	40 cm (15.7 in )

A rule of thumb generated by RMEP experience is that, for two-wheeled vehicles, a given obstacle can be climbed if the wheel diameter is three times the obstacle height, provided that due consideration is given to the frictional interface, tire deformation, and a positive means for surface engagement, e.g., cleats, cups, teeth, or other aggressive tread elements. (A vehicle with four powered wheels, of the same type used in the two-wheeled vehicle, might negotiate a given obstacle with smaller wheels if it were properly arranged and articulated. An example is illustrated in Figure 2.)

In the present instance, four wheels smaller than 30 or 40 inches in diameter would not satisfy the clearance requirements, but going to a slightly larger diameter, 36 (or 48) inches, would enable a two-wheeled vehicle not only to clear, but to climb over, the specified obstacle height. With the wheels thus sized for a two-wheeled vehicle, it can be designed as such, with the attendant advantages of less external

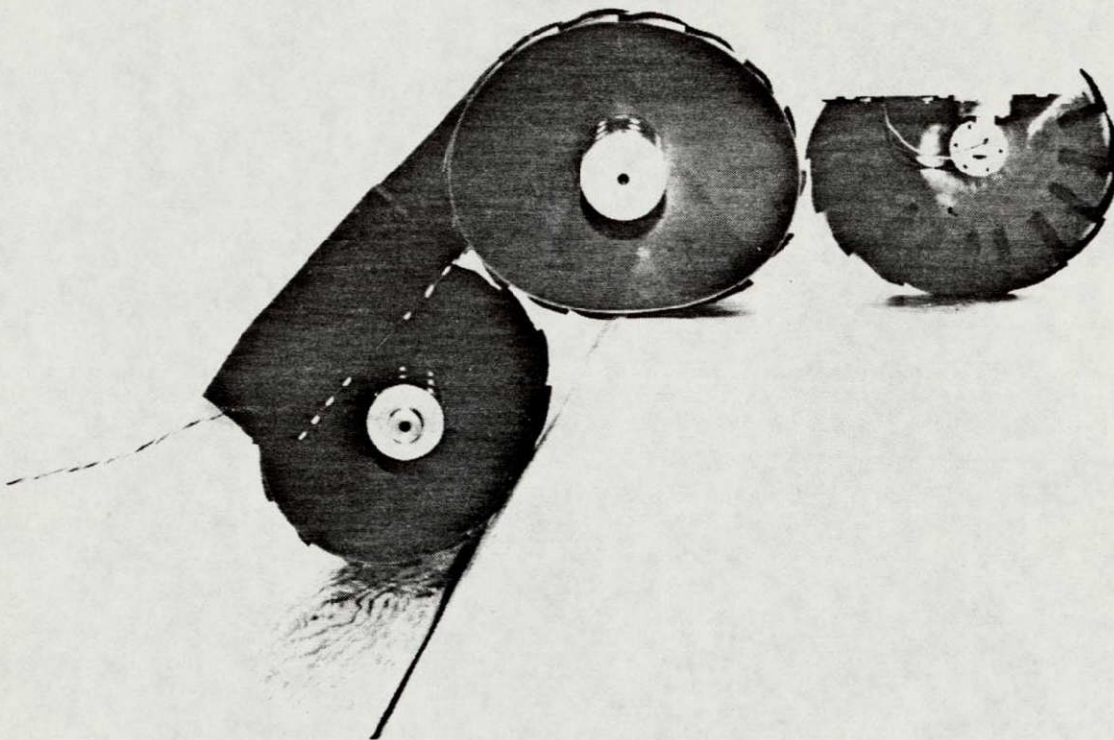
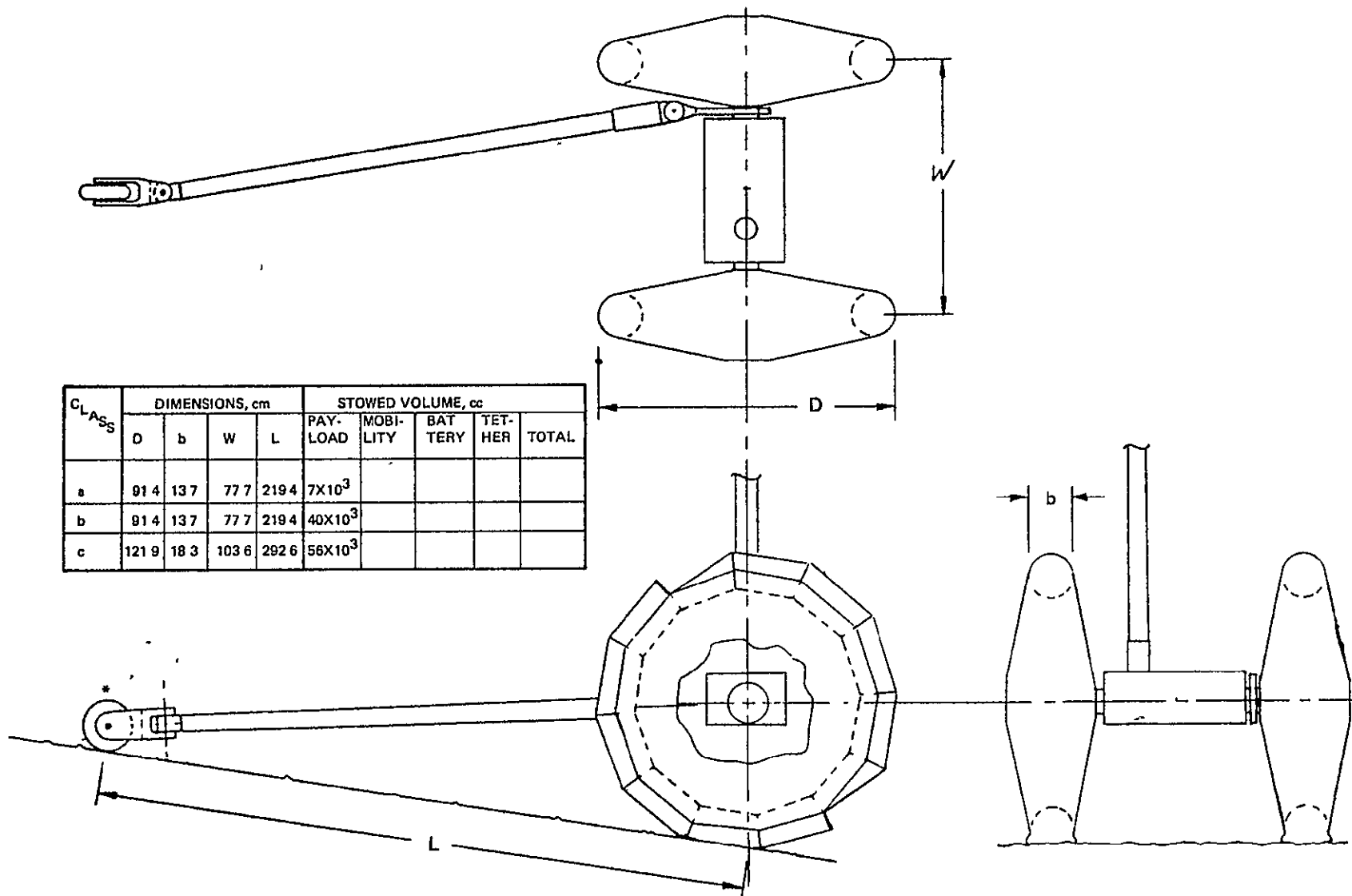


Fig. 2 Grumman's Remote Controlled Tactical Vehicle (RCTV)

resistance and easier packaging and pumping requirements than a four-wheeled vehicle of the same total mass.

Finally, for this study, torus cross section diameter, tire-to-hub membrane geometry, and wheel spacing were established by using the proportions of the RMEP wheel wherever possible. The only exceptions occur for Class b and c vehicles at low wheel inflation pressure, where the torus cross section diameter must be increased to provide adequate pneumatic load to support the vehicle.



\*CONTACT FOR TAIL BOOM IS STILL TO BE DETERMINED - WHEEL SHOWN IS SCHEMATIC

Fig. 3 General Arrangement MMR

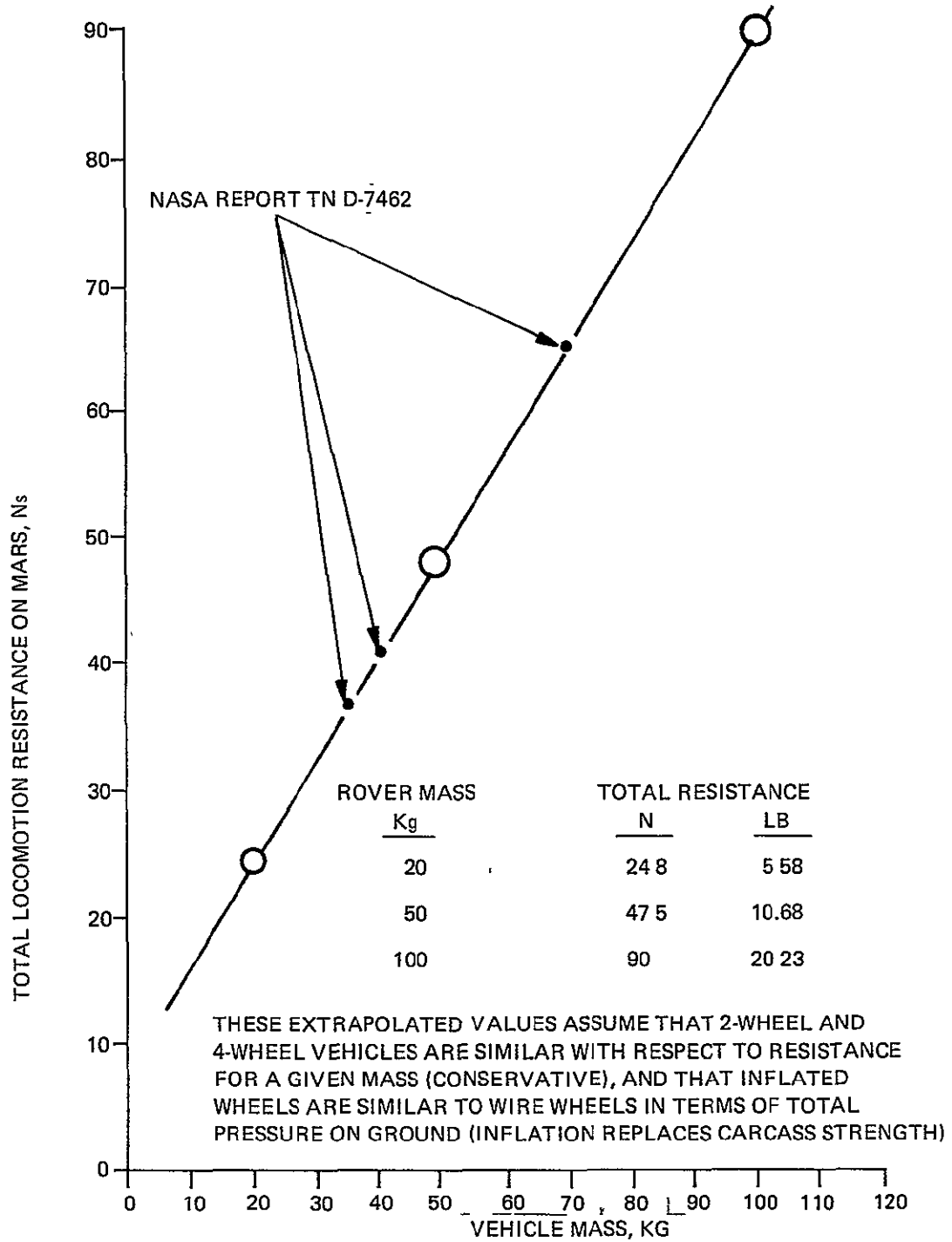


Fig 4 Approximation of Vehicle Total Locomotion Resistance Vs Mass

For a rigid wheel, the external resistance is given by:

$$R_E = 1 / \left[ (3-n)^{2n+2/2n+1} (n+1) (k_c + bk_\phi)^{1/2n+1} \right] \left[ 3W/(D)^{1/2} \right]^{2n+2/2n+1}$$

where

- $R_E$  = external resistance per wheel (N)
- $n$  = sinkage exponent (1)
- $k_c$  = cohesive modulus of deformation (0.1 N/cm<sup>2</sup>)
- $b$  = wheel width (cm)
- $k_\phi$  = friction modulus of deformation (0.27 N/cm<sup>3</sup>)
- $W$  = vertical force on wheel (N)
- $D$  = wheel diameter (cm)

In Reference B the external resistance is calculated using a formula which applies for a low ground contact pressure. Both that formula and the rigid wheel formula given above can be found in Reference C.

Results for various slopes, at inflation pressures of 0.5 and 2.0 psi, are given in Table 3. Except for the higher slopes, the total resistance of any of the three two-wheeled vehicles is approximately equal to, or less than, the value read from Figure 4. Therefore, the total energy calculations in this section which make use of Figure 4 values are reasonable.

### 2.3 REVERSING TRAVEL

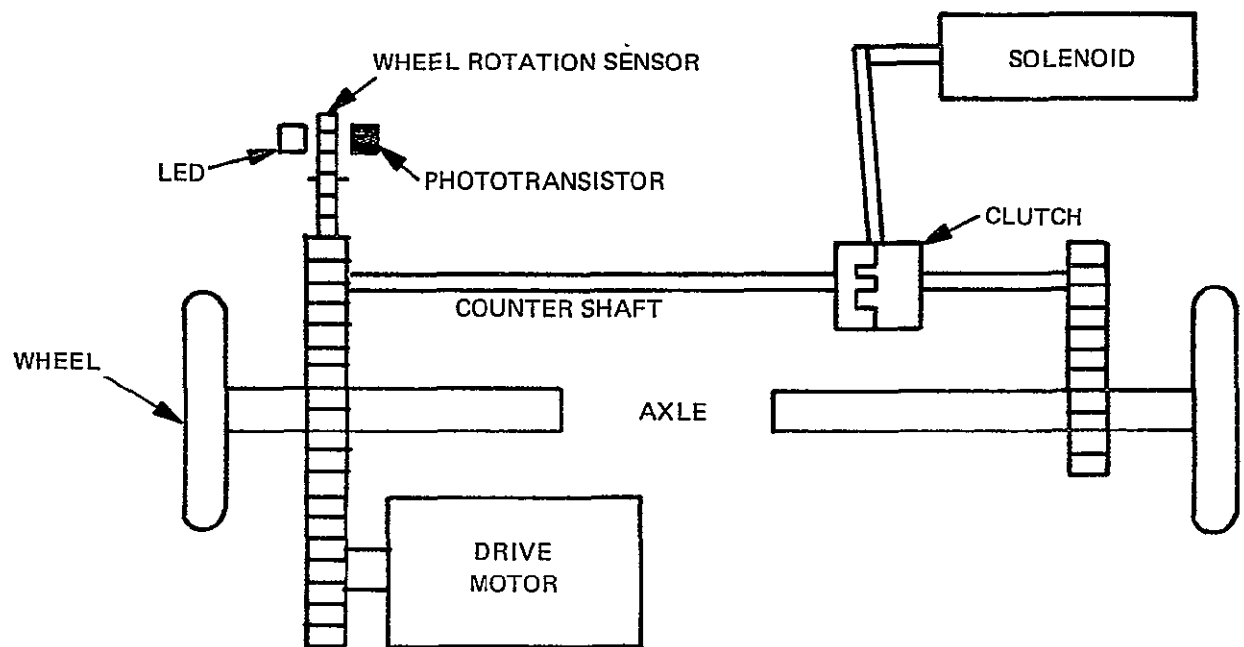
The other mobility question addressed in this study was how to provide short distance reverse travel. The drawback of a two-wheeled vehicle with trailing boom is that it cannot be backed away from contact with a large obstacle simply by reversing wheel rotation, since the boom would no longer resist the reaction torque, but would instead flip itself and the payload over to the opposite side of the axle.

The RMEP reversed travel direction by pivoting the vehicle using differential wheel rotation (Figure 5). If the MMR vehicle inadvertently runs up against a large, insurmountable obstacle, it may not be possible to retreat by pivoting. In this event, a direct reversing maneuver would be required for a short distance.

To prepare for reverse travel, the tail boom must be flipped over to the opposite side without appreciably rotating the payload. The c.g. of the total vehicle must also cross over the axle. The latter requirement dictates that the c.g. of the payload alone must be quite close to the axle.

TABLE 3 TOTAL LOCOMOTION RESISTANCE ON MARS, NEWTONS (LB-FORCE)

VEHICLE MASS, kg	SLOPE, deg	INFLATION PRESSURE, psi	
		0.5	2.0
100	20	162.68 (36.57)	198.8 (44.69)
	5	63.13 (14.19)	99.25 (22.31)
	0	29.09 (6.54)	65.21 (14.66)
50	15	67.08 (15.08)	72.43 (16.39)
	5	33.46 (7.52)	39.31 (8.84)
	0	16.40 (3.69)	22.25 (5.06)
20	15	30.49 (6.85)	31.37 (7.05)
	5	17.07 (3.84)	17.96 (4.04)
	0	10.27 (2.31)	11.25 (2.53)



**SENSOR.**

- FINE – 3½ IN. DRIVE  
– 12° STEER
- COARSE – 63 IN. DRIVE  
– 216° STEER

**MOTOR.**

- 40 RPM – NO LOAD
- 24 LB-FT- STALL
- 0.1 HP

**Fig. 5 RMEP Wheel Drive System**

Two candidate techniques to prevent payload rotation during boom flipover should be investigated:

- A. Deflate the MMR's wheels so as to have the chassis contact the surface
- B. Extend one of the surface experiments (e.g., drill, seismic package) to stabilize the chassis.

In either case, the boom must be uncoupled from the chassis and rotated approximately 180 degrees around the axle. An approach using the drive motor itself is described in Subsection 3.3.

Figure 6 is a schematic of the reverse travel sequence using wheel deflation/reinflation. After backing away from the obstacle only far enough to gain maneuvering room, the boom flip-over sequence would be reversed so that the vehicle is again facing in the original direction of travel. This is particularly important where an umbilical is involved.

#### 2.4 REMOTE COMMAND

Remote command capability (Table 4) built into the RMEP is directly applicable to the MMR vehicle. Figures 7 and 8 depict the mobility hardware that implements the remote commands.

TABLE 4 REMOTE COMMAND CAPABILITY

COMMAND	FUNCTION
DRIVE	● VEHICLE GOES FORWARD 3 1/2 IN./COUNT
STEER	● VEHICLE TURNS CW 12 <sup>0</sup> /COUNT
REVERSE	● VEHICLE BACKS UP OR TURNS CCW
COARSE	● DRIVE & STEER ARE 18 TIMES GREATER
MAST-	● MAST GOES UP
DOWN	● MAST GOES DOWN
PUMP	● WHEELS INFLATE
DEFLATE	● WHEELS DEFLATE
(RESET)	● ALL MOTORS STOP

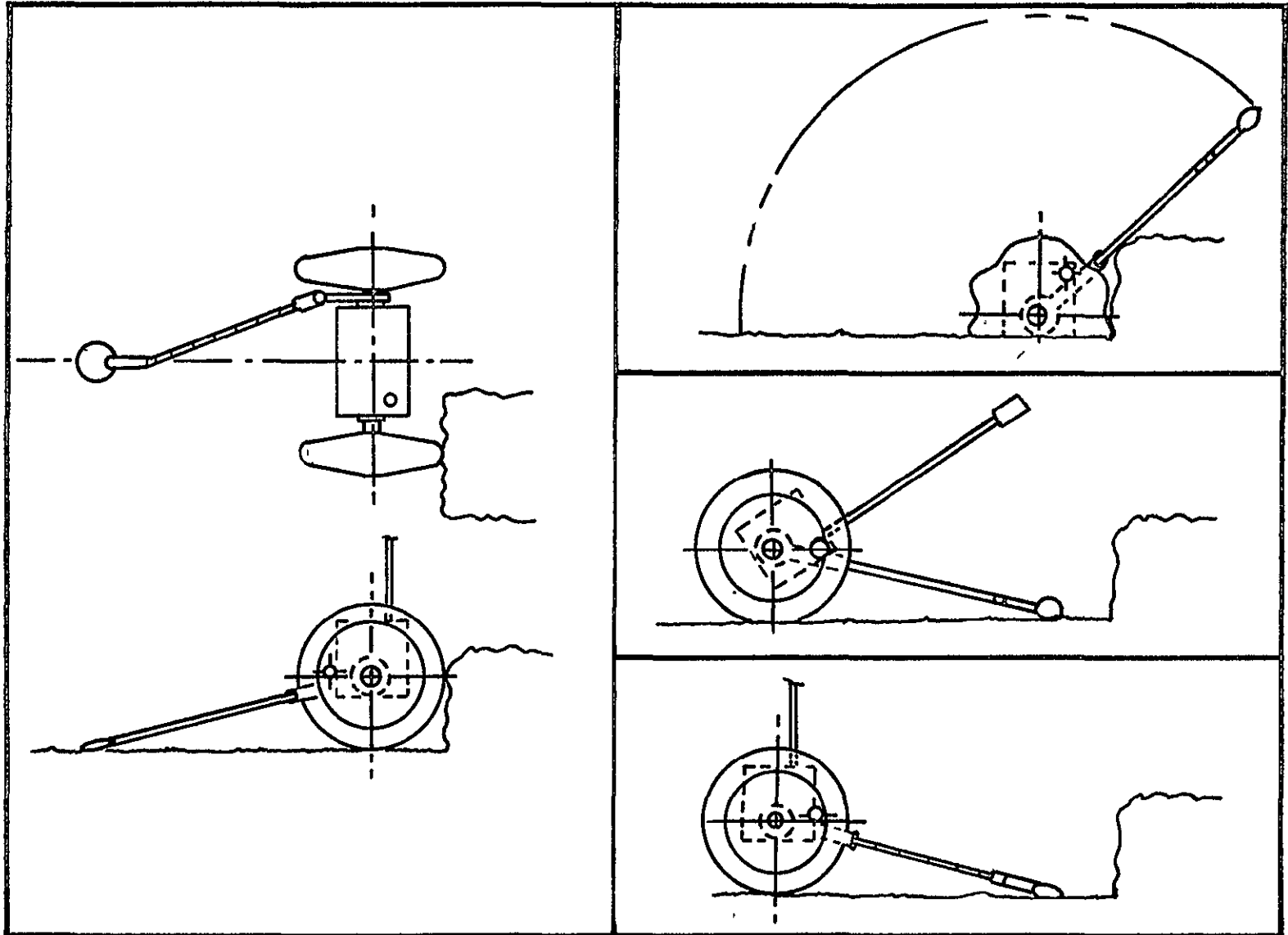


Fig. 6 Suggested Sequence for Reverse Travel

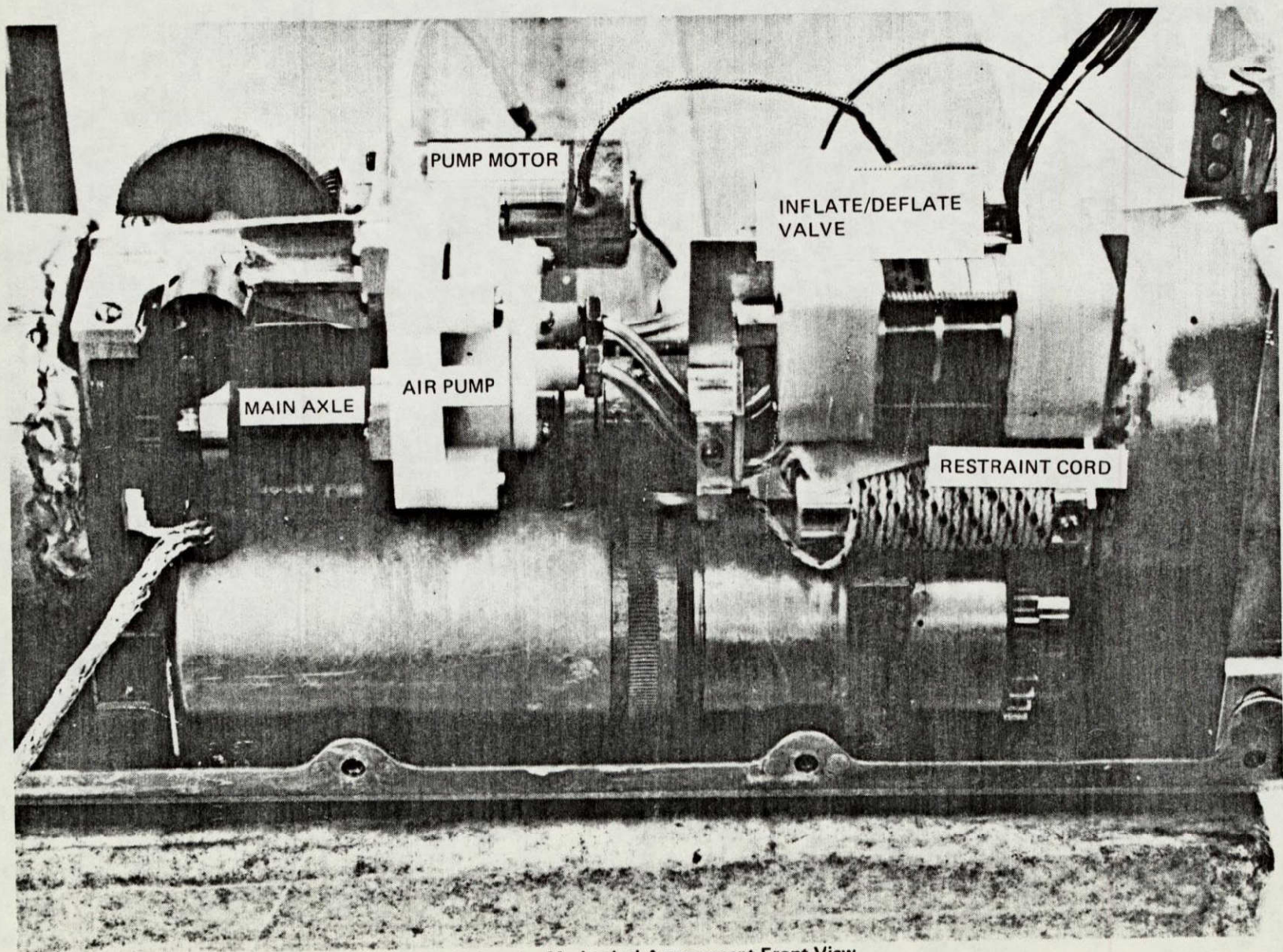


Fig. 7 Interior Mechanical Arrangement-Front View

2504-011

15

ORIGINAL PAGE IS  
OF POOR QUALITY

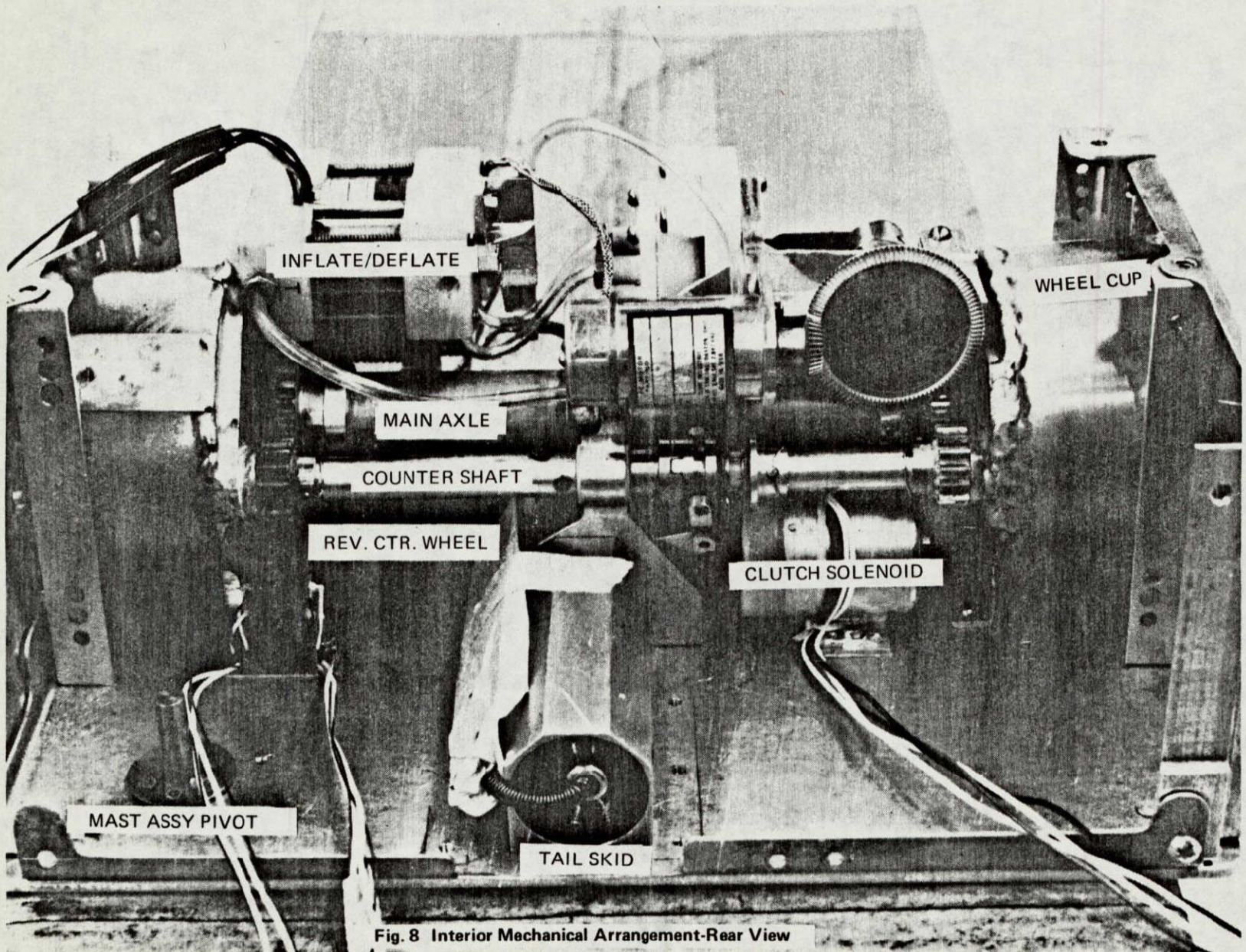


Fig. 8 Interior Mechanical Arrangement-Rear View

ORIGINAL PAGE IS  
OF POOR QUALITY

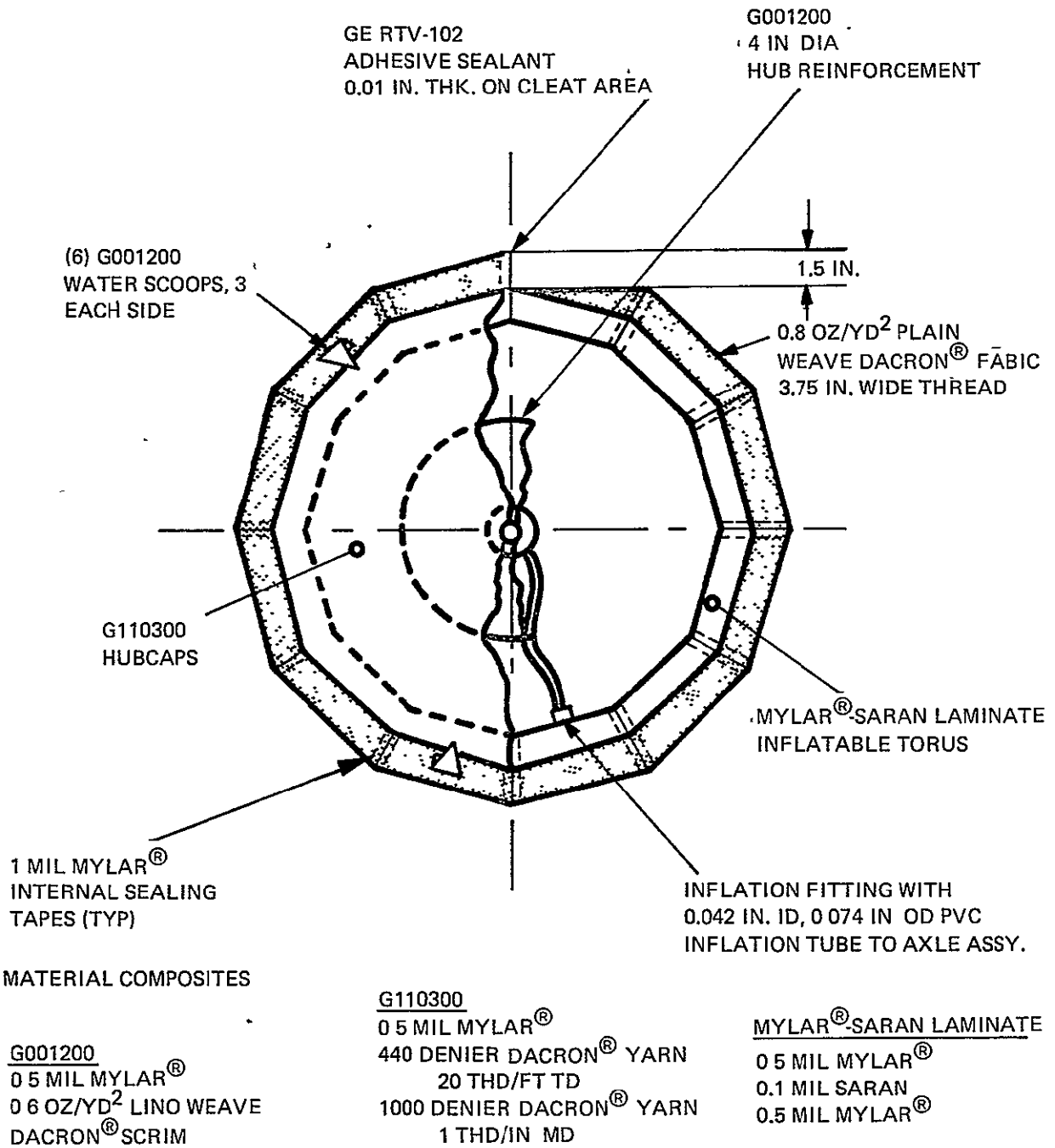


Fig. 9 Inflatable Toroidal Wheel Configuration (Prepared by G.T. Schjeldahl Co.)

be found in Reference D. The basic design of the MMR wheel will follow that of the RMEP with the possible addition of another cleat facing in the opposite direction to assist during backup maneuvers.

The pressure in the RMEP wheel was 3 psi gage. For the Mars mission it may be desirable to greatly reduce the inflation pressure, perhaps to 0.5 psi. This would not only reduce the energy required for each inflation-deflation cycle, but would also prevent the inflated wheels from sinking and producing the high rolling resistance associated with rigid wheels in weak soil, assuming the allowable ground pressure of 0.5 psi as has been speculated. In the NASA report, Reference A, the wheel pressure on the ground was  $0.517 \text{ N/cm}^2$  (0.75 psi), provided in that case by carcass stiffness rather than inflation.

#### Power Considerations for Wheel Inflation

When inflating the wheels, two parameters known to be important regarding the attendant electrical energy requirements are: a) the wheel diameter, in particular the inflatable volume, and b) the inflation pressure above ambient. The variation of the work required for inflation with respect to these parameters is shown in Figure 10, normalized to the 20-inch diameter wheel. It is apparent that a low inflation pressure is desirable, especially for the larger wheels. This figure assumes that all wheels have the same relative proportions as the 20-inch wheel.

A low pressure torus would not present any fundamental structural design problems. For example, the webs could be strengthened near the hub to minimize windup. A 36 x 5.4-inch wheel could support the 20 and 50-kg vehicles at 0.5 psi; however, for the 100-kg vehicle, the torus diameter must increase to approximately 7.5 inches. For all vehicles, the side loading (side hill running) problem needs further study.

For wheel sizes up to about 50 inches in diameter (D), the wheel proportions for a light MMR are expected to remain constant. For example, at  $D = 20$  inches, the wheel tread (T) will be 3 inches; for  $D = 40$ ,  $T = 6$ . By keeping  $D/T$  constant, the volume of the wheel that must be inflated varies as  $D^3$ . Since the inflation pressure is expected to remain constant, a single curve can be used to estimate the work required for an inflation/deflation cycle as a function of D. This is shown in Figure 11, normalized to  $D = 20$ .

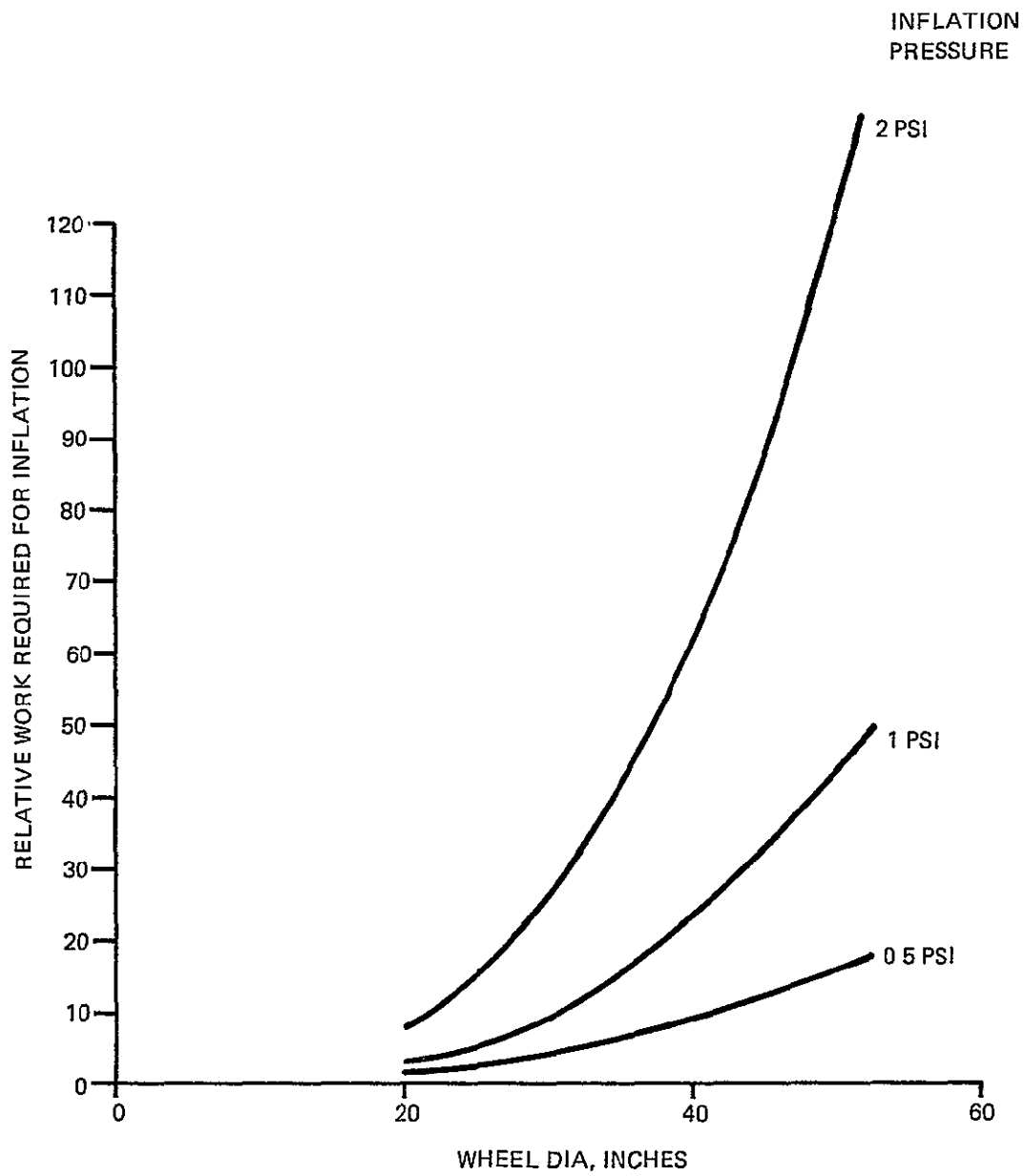


Fig. 10 Relative Work Required for Wheel Inflation at Different Pressures

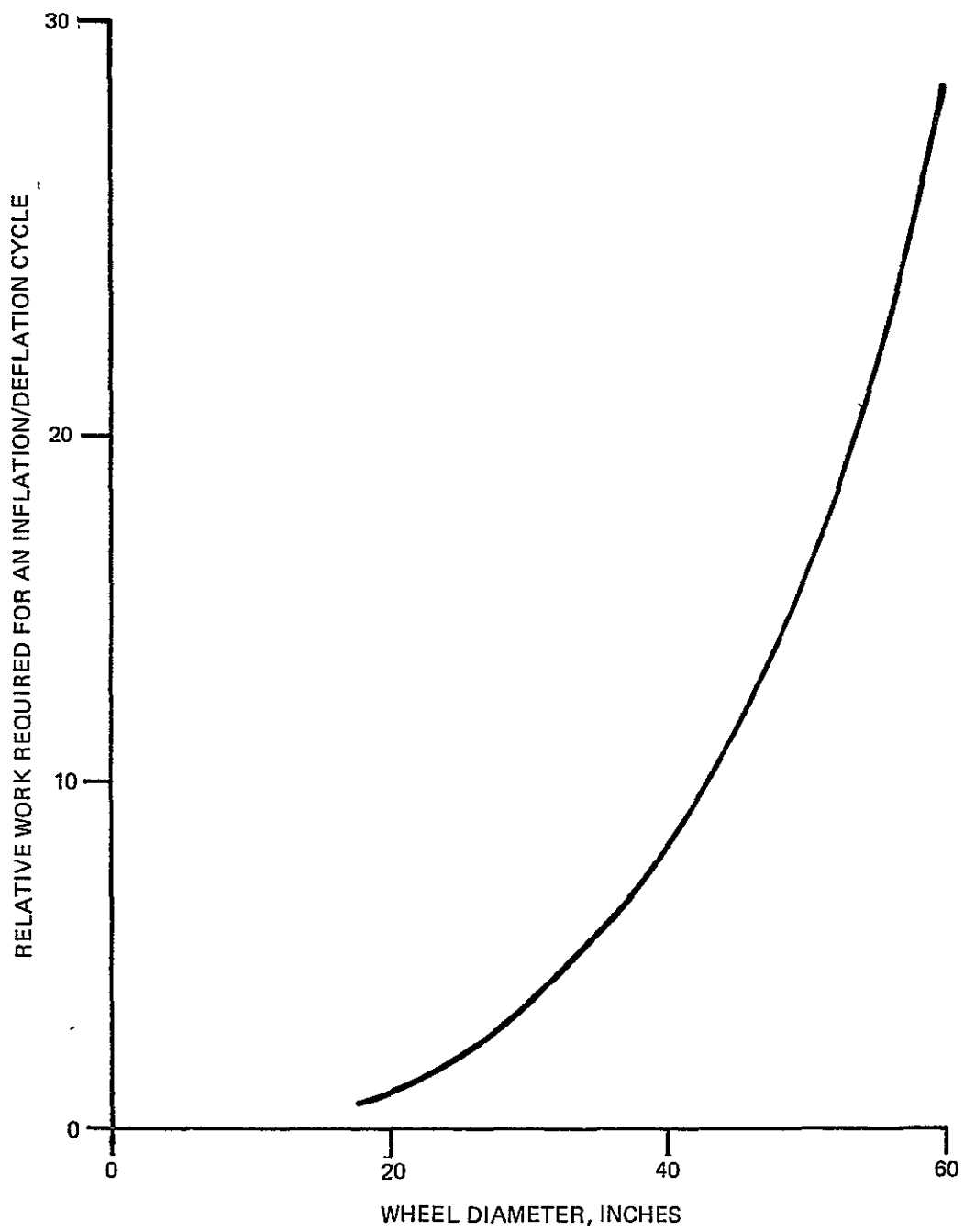


Fig. 11 Relative Work Required for Wheel Inflation for Different Wheel Sizes

There is however, a limit to the weight (W) that a given T can support for the proposed inflation pressure, 0.5 psi. Since D is determined primarily from the obstacle size to be negotiated, a larger T can be expected for a MMR when W exceeds the relationship:  $W < \frac{\pi}{4} T^2$  (W is in pounds, T is in inches). The work required for an inflation/deflation cycle for a constant D, as a function of T, is shown in Figure 12, normalized to T = 3.

It is expected that the MMR wheel will be about 45 percent heavier than an equivalent sized RMEP (2 ounce) wheel. This is because of the extra shielding required for protection against uv radiation and other minor design changes. A uv shield would be an additional layer of a thermoplastic polyester elastomer, possibly Hytrel™, covering all surfaces of the wheel. The anticipated rate of increasing wheel weight as a function of diameter is shown in Figure 13, normalized to the 20-inch wheel. The stored volume also will increase at about the same rate since the densities of the various materials used to construct the wheel are all about the same.

To increase the life of the wheel on the relatively rough surface of Mars, an extra layer or layers of protective material such as Hytrel™ may have to be added to the tread. Hytrel™ is a good candidate since it has the necessary low temperature flexing capabilities. It is expected that the tread weight will increase by a factor of 1.7 every time the tread life is doubled, and the tread weight represents approximately 36 percent of the entire wheel weight. It is not possible at this time to determine to what extent the tread life has to be extended, but a nominal increase in the weight may result.

### 3.2 TAIL EXTENSION

The tail boom is required to provide a third ground contact point for stability, including the reaction of wheel drive torque. The four-foot long boom is a stacer which starts out compressed into a cylinder approximately 2.5 inches long by one inch in diameter. The stacer is a coiled strip of thin gauge stainless steel which uncoils and extends irreversibly when released. A restraint cord stowed in the outboard end pays out down the center of the resulting tapered tube to restrict the extension, keeping sufficient coil overlap to maintain the required bending strength. The outboard end cap also supports a castering wheel to minimize drag and side loads on the boom during maneuvers. The inboard end of the stacer is attached to the case which is fastened to the flip-over mechanism.

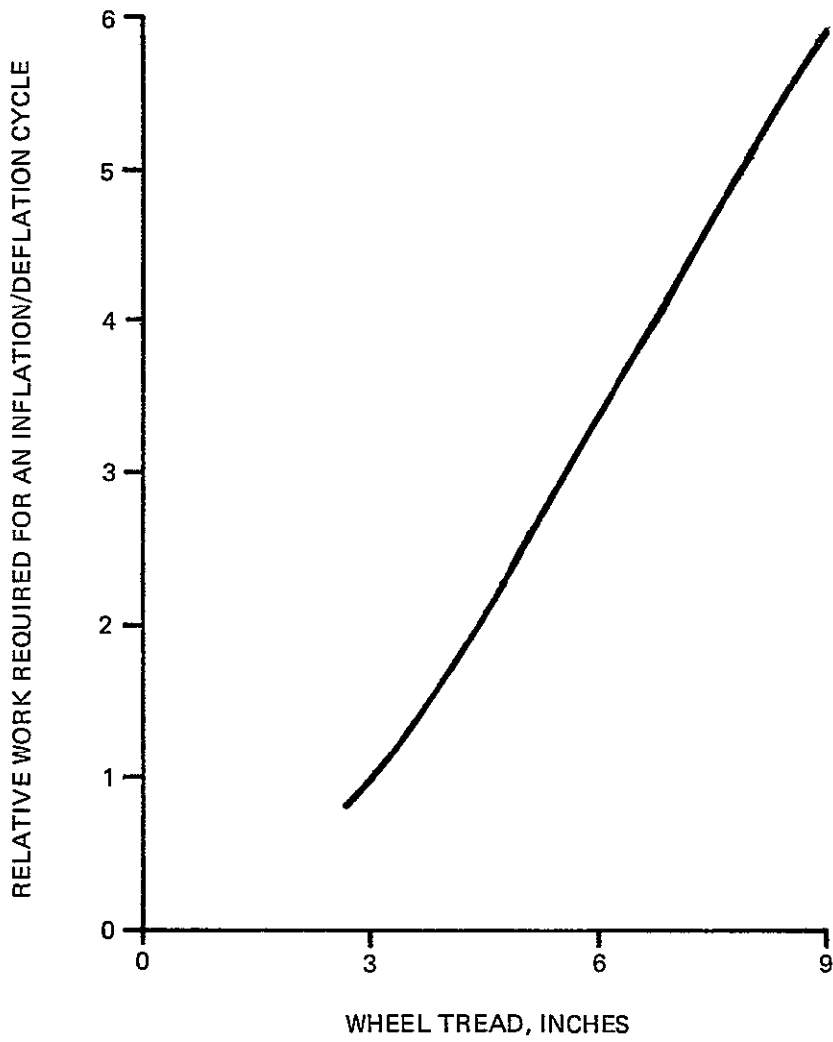


Fig. 12 Relative Work Required for Wheel Inflation for Different Tread Sizes

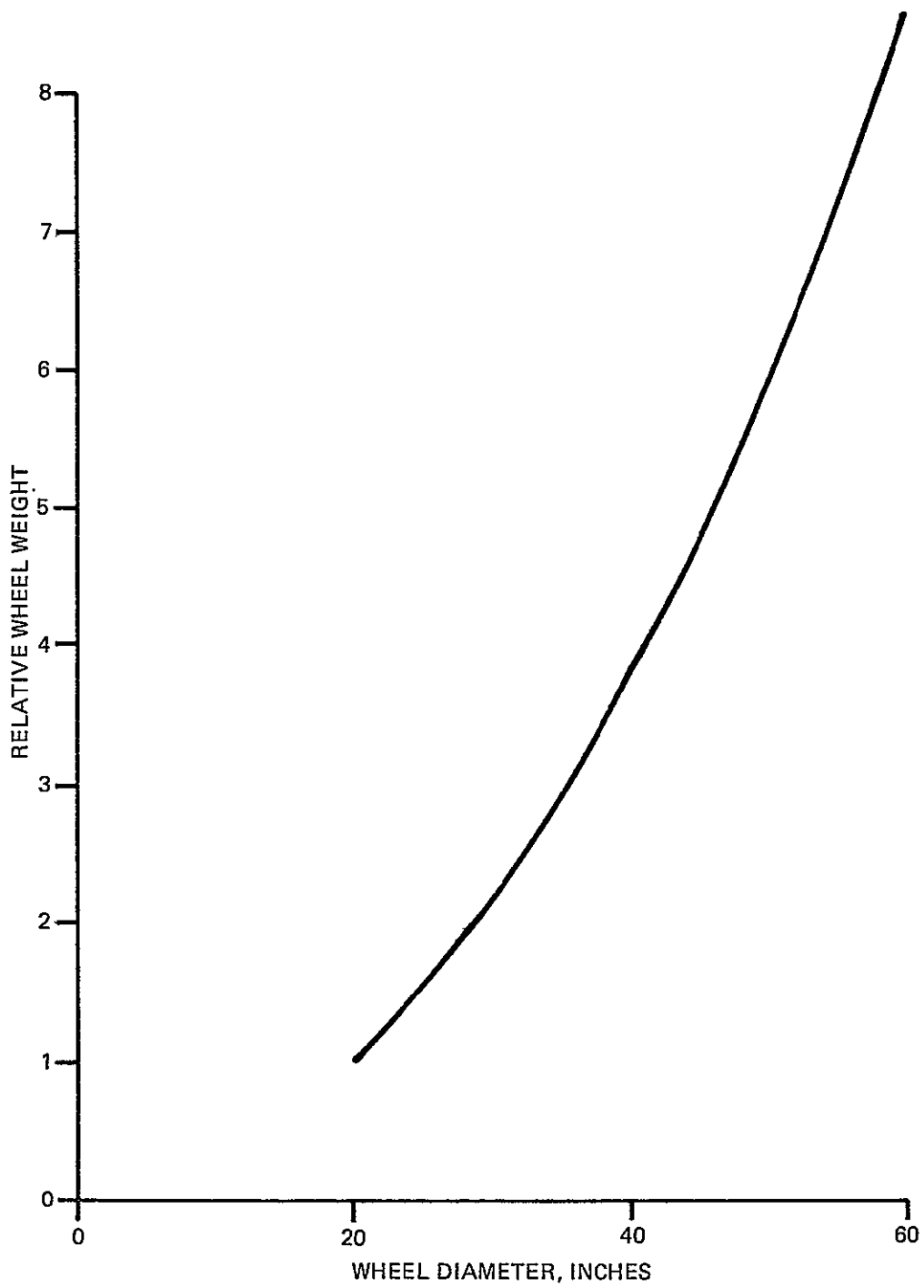


Fig. 13 Relative Wheel Weight As a Function of Wheel Diameter

### 3.3 FLIP-OVER SYSTEM

During normal operation, the tail boom must be fixed to the chassis to provide resisting torque. However, when a reverse travel maneuver is required, the tail boom must be uncoupled so that it can be swung over to the forward side of the vehicle without rotating the payload. Fixing and uncoupling are inherent if an irreversible gear train is used to connect the boom to the motor used to flip it over. The wheel drive motor could be used to flip the tail boom if a gear changer, perhaps a solenoid actuated splined shaft, were used to shift the motor output from the wheel drive to a gear train leading to the boom; see Figure 14. During the design phase, this approach would be compared with a separate flip-over motor. In any case, the payload must be prevented from rotating, either by extending an experiment or deflating the wheels.

It is expected that tail boom flip-over and reverse travel will only be used for short distances to back away from an obstacle which prevents a "U" turn. By thus limiting reverse travel and by preventing payload rotation, no adverse effects on either the payload or the umbilical cable are expected.

### 3.4 TETHER PAYOUT DEVICE

Using a tether, or umbilical, to feed electrical power to a Class a or b MMR would present the same design problems with the RMEP concept as with any other configuration, except that with the RMEP concept there is a possibility of fouling with the tail boom. The boom castering wheel assures that boom-to-ground contact will always be rolling, whether the boom is trailing or slewing, and rolling over the cable should cause no problem.

The umbilical payout port is near the center of the rear face of the chassis to minimize disturbance torques as the umbilical is withdrawn. The payout umbilical will, therefore, be close to the tail boom and castering wheel. It will not necessarily lie flat on the ground; it may have an irregular helical shape from being coiled in its container. Detail design of the wheel and caster fitting must preclude any tangling or pinching of the cable. Also, the umbilical must be prevented from riding up on the boom by suitable deflecting shields.

The payout device itself might involve pulling off from the outside wrap of a rotating reel - either a pancake or a long cylindrical shape - with just enough drag

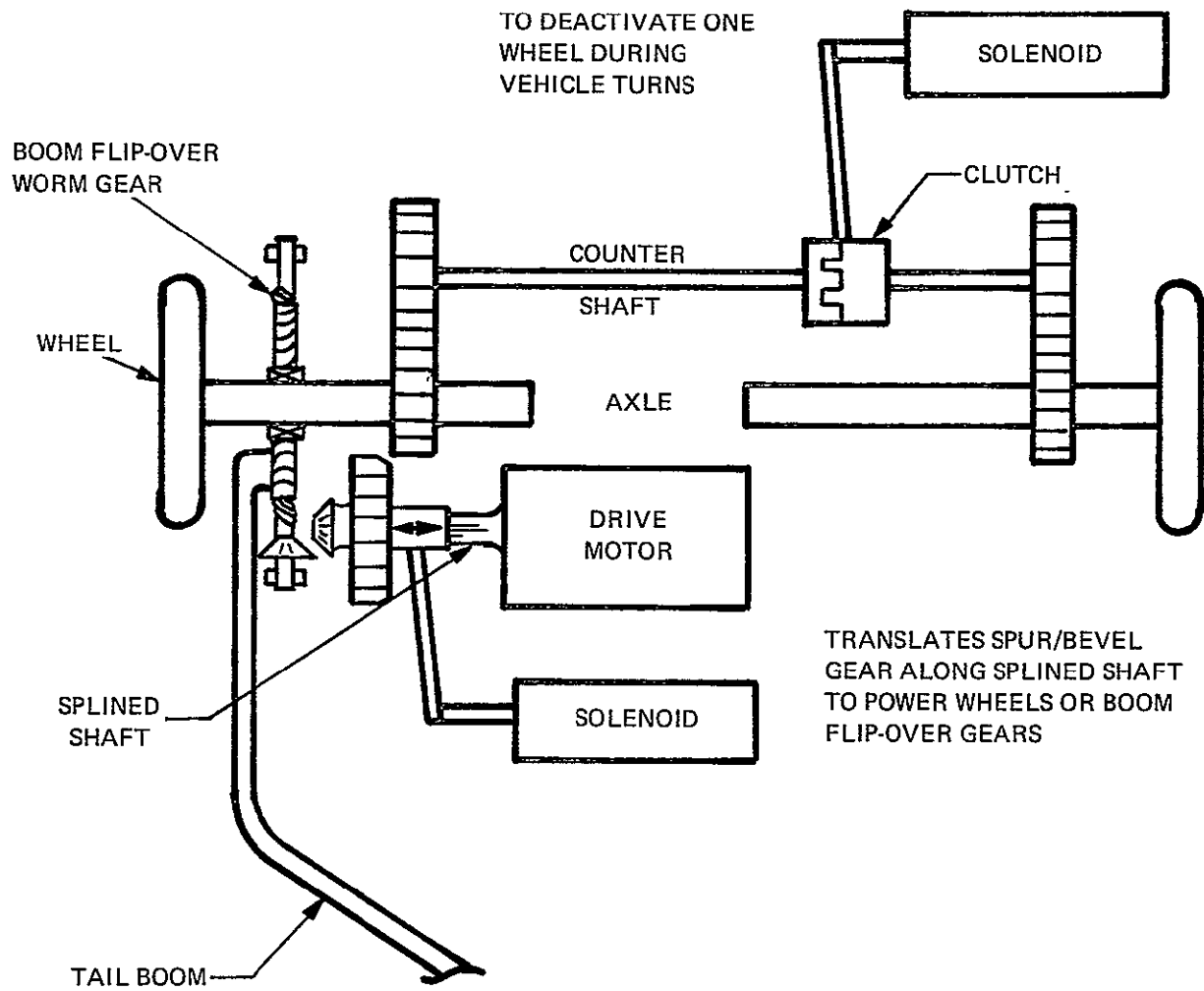


Fig. 14 Possible Boom Flip-Over Mechanization Using Wheel Drive Motor

built into the hub to prevent unwanted free running. Another approach is to pull the cable out from the center of a coil or a "fire hose" packing configuration. Each approach has minor advantages and drawbacks; none was studied in detail.

Figure 15 shows a coil pulled from the center through a cone-shaped exit. It involves no moving parts, requires a constant, small pull regardless of how much cable has been used, does not put severe bends in the cable, and has a low probability of jamming inside the can. If a surface coating is used to provide tackiness for maintaining coil shape, it must not be affected by temperature extremes.

### 3.5 HAZARD DETECTION & AVOIDANCE SYSTEM (HDA)

The hazard detection and avoidance (HDA) subsystem protects the MMR on a real-time basis and provides non real-time data to aid the remote operator. Vehicle protection is accomplished by automatically stopping the rover prior to physical encounter with adverse mobility conditions or immobilization by weak soil. Hazard avoidance is accomplished by providing information on hazard type and location to the remote operator to assist in driving decisions.

The primary HDA subsystem requirement is to prevent the remotely controlled rover from unintentionally damaging or immobilizing itself. The detailed subsystem requirements are related to the ability of the MMR to withstand impact with certain types of surface features, its ability to decelerate, and the extent to which it can move into soft soil and extricate itself.

The generalized HDA subsystem's elements and interrelationships are shown in Figure 16. It is independent of external illuminating conditions. This allows the mission a degree of freedom in movement for all light conditions. The HDA subsystem serves to back up and/or confirm the MMR's imaging device.

Grumman has conducted sensor investigations in the area of hazard detection and avoidance for lunar excursion vehicles. The relatively simple sensor approaches discussed in the following sections are considered to be worthwhile candidate sensors for the small, slow-speed MMR. Grumman has also designed Hazard Detection and Avoidance Subsystems utilizing optical and RF Radars/Processors that are more complex than those required for the slow-speed MMR's (see References H, I and J).

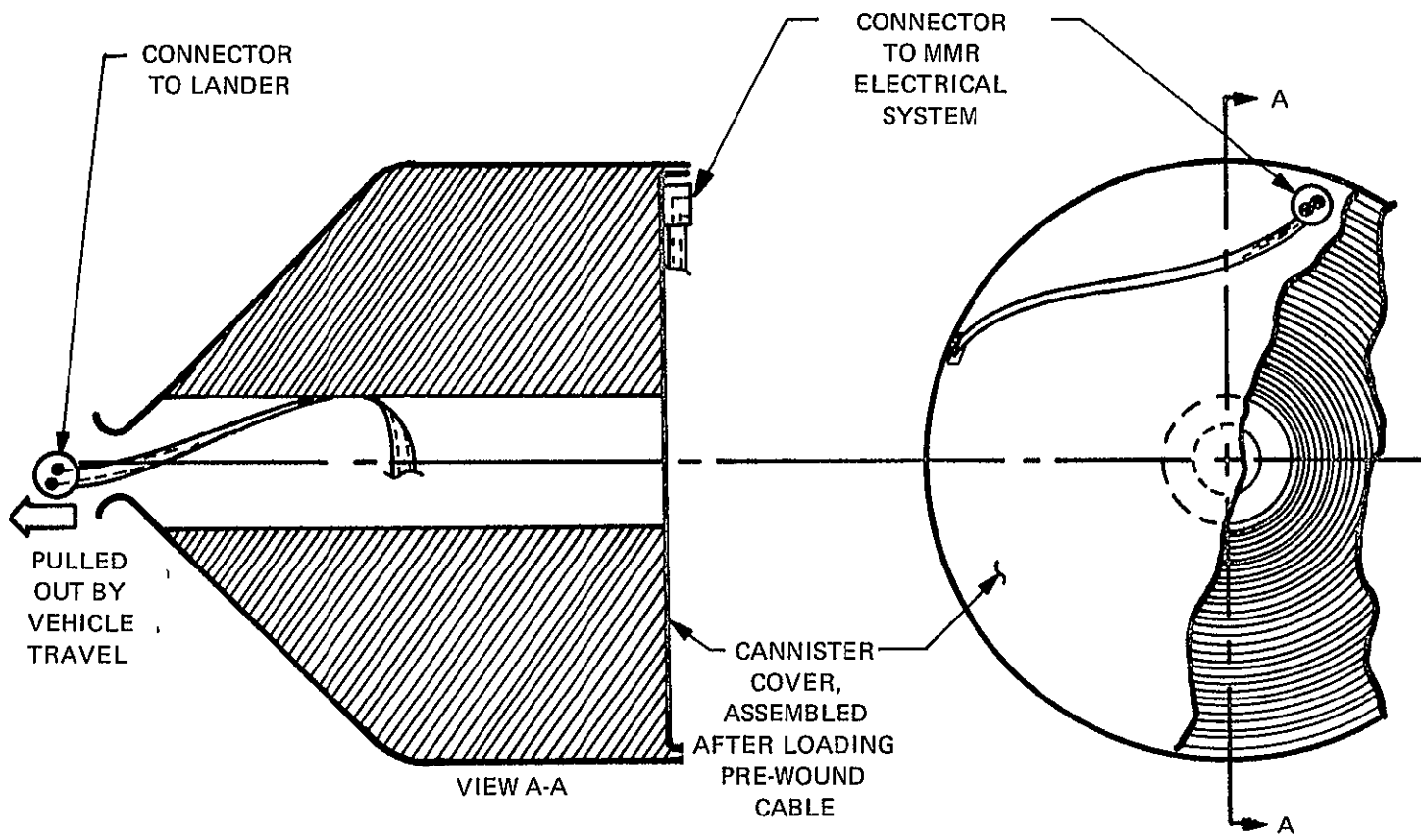


Fig. 15 Possible Umbilical Payout Concept (No Scale)

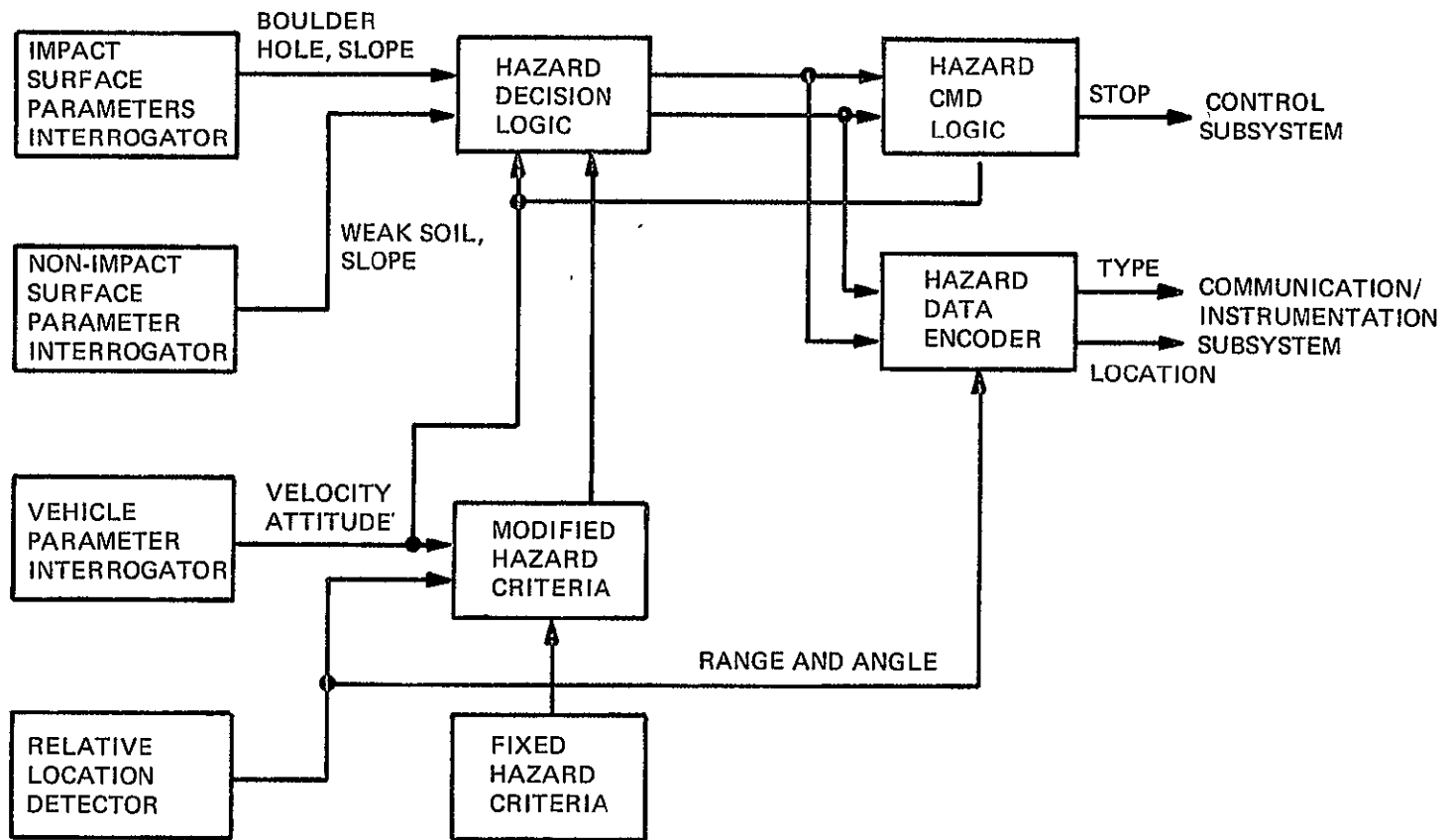


Fig. 16 Hazard Detection & Avoidance Subsystem Functional Block Diagram

### 3.5.1 Mechanical Hazard Sensor

One candidate HDA uses a mechanical sensing system for obstacle avoidance. This approach requires a device connected to the vehicle, carrying its sensing point ahead of the vehicle a distance at least as great as the required stopping distance of the vehicle. The connection to the vehicle must be capable of collapsing without damage through this distance, as the vehicle stops, and extending itself again as the vehicle backs off and resumes forward travel in a new direction. The sensor must also sense holes and crevasses, operate on up, down, or side grades, and not be fooled by changes in slope.

The worst case stopping distance required after receipt of a "stop" signal is negligibly small. The attendant calculations considered the vehicle mass, velocity, Martian gravity, friction between wheels and soil, and possible downhill slopes. For the speed of 0.1 km/hr, the stopping distance is estimated to be less than one inch.

An example of a device to sense obstacles (not holes or crevasses) would be a horizontal bar across the front of the vehicle, suspended on a simple collapsible scissors linkage, Figure 17. The linkage would hold the bar a distance in front of the vehicle somewhat greater than the required stopping distance, and at a height above the ground such that the bar would clear and pass above obstacles which the vehicle could negotiate, but would contact higher obstacles. The scissors linkage would collapse to permit the bar to move toward the vehicle when contacting an obstacle, while maintaining the bar at a constant height above the ground. Initial collapsing motion would shut the drive motor off and also apply the vehicle brakes (if required at all). Springs, preloading the linkage to the full forward position, would absorb the contact energy, and also provide automatic no-power-required redeployment to the normal sensing position when the vehicle backed away from the obstacle. It might be necessary to incorporate automatic bar-height control slaved to vehicle pitch attitude to compensate for grades. Vehicle attitude would be measured by gravity sensors such as bubble switches/inclinometers.

The requirements for hole and crevasse sensing are more severe than for obstacle sensing. One obvious difference is that the hole sensor must contact the surface continuously with a sliding or rolling probe(s). A finite amount of power is required to overcome the probe friction at all times, even on completely level terrain. The hole sensor should also be able to evaluate the span of the hole, that is, the distance

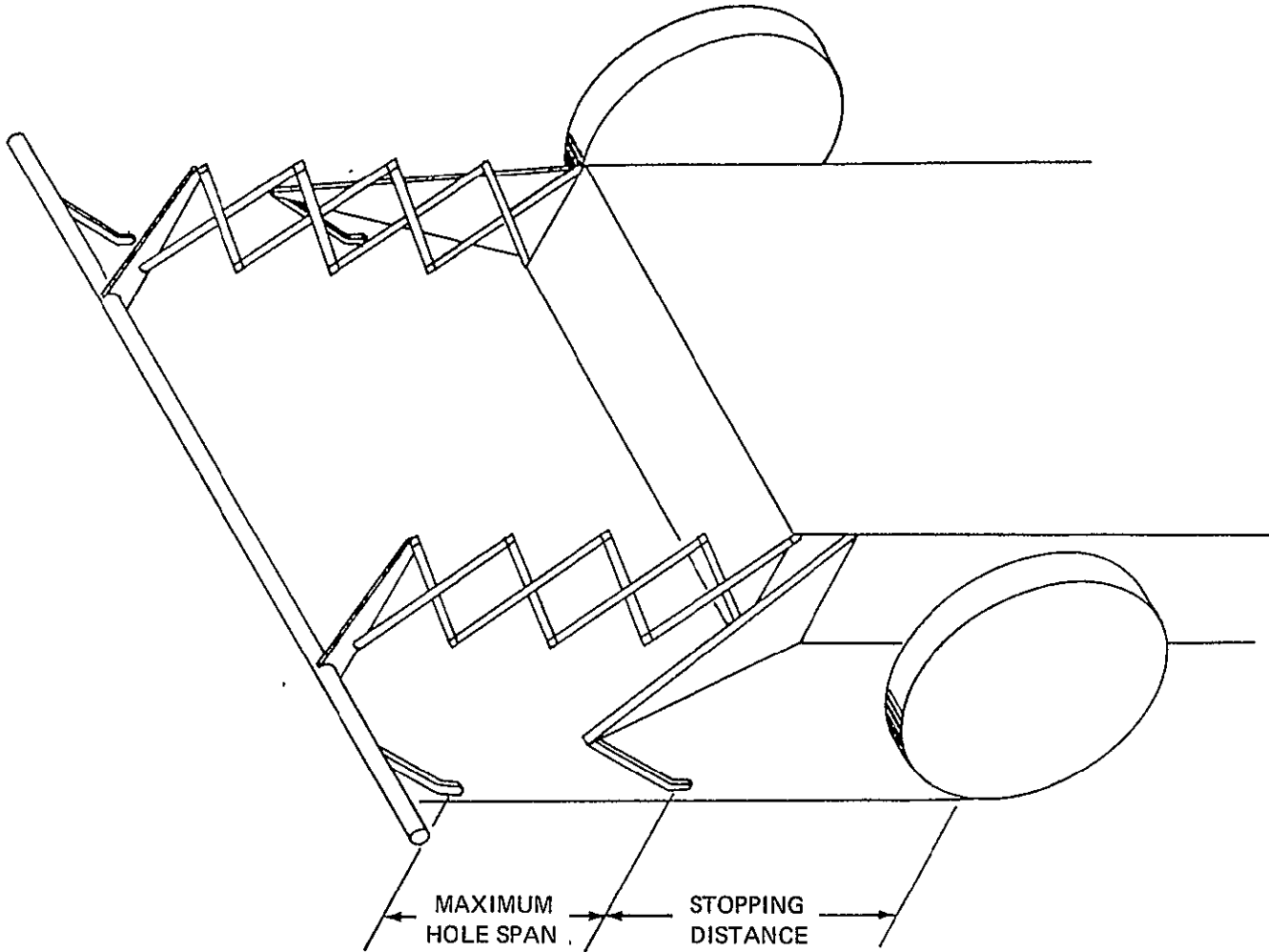


Fig. 17 Mechanical Bumper (No Scale)

to the far side, as well as the depth, so that the vehicle is not stopped unnecessarily by a narrow or shallow crevasse which it could easily bridge across or drive into and out of.

It appears possible to add a hole-sensing system to the obstacle sensing arrangement suggested above. A pair of small sensing skids or wheels on trailing arms would be arranged so that one skid/wheel is approximately under the bar (attached to the bar), and the second directly aft of the first, attached to the vehicle. The fore-and-aft distance between the skids would be slightly smaller than the maximum hole-span which the vehicle could negotiate. A signal to apply the vehicle brakes would come from both skids dropping to full extension. This would indicate a hole too wide and too deep to be negotiated.

This arrangement would require that the obstacle-sensing bar be relocated farther forward than on the configuration for obstacle-sensing alone, in order that the rear sensing skid could still be forward of the vehicle at a distance greater than the stopping distance. It would probably be desirable also to use two pairs of skids/wheels, one pair forward of each front wheel. Further investigations are necessary with regard to stowability and reliability of this candidate hazard detector.

### 3.5.2 Optical Techniques

There are basically three optical methods that terrain obstacles can be detected with: direct ranging, loss of return by interruption of beam path, or return from obstacles. The latter two approaches will be referred to as optical triangulation. These triangulation schemes require no complex ranging or correlation as they intrinsically range and detect obstacles. One technique is based on Bionic Instruments, Inc., Laser Cane which is a mobility aid for the blind. (Bionic Instruments has accomplished a study entitled, "Feasibility Study of a Hazard Locator for LRV," February 1970, NAS 8-24901.) In about the same time frame after consulting with Bionic Instruments, Grumman performed a preliminary design of a LRV Hazard Detector using the same principle. As part of a future study, the LRV design could be repeated constrained by the MMR's more modest requirements (slow speed). The Grumman preliminary design of the LRV Hazard Detector appears in the Appendix.

## Section 4

### MOBILITY & CONTROL SUBSYSTEM

Data in Figure 4 indicate total vehicle tractive force requirements of 5.58 pounds, 10.68 pounds, and 20.23 pounds for vehicle Classes a, b, and c, respectively. The existing RMEP drive-train power rating is more than ample to transport all three classes of vehicles. What will be required is selection of a motor rated at a lower speed to match the reduction from an RMEP speed of 1.6 km/hr to the MMR speed of 0.1 km/hr. For Class c operation there will be an increase in the gear box size and weight. The Class b vehicle will require a lesser gear box size increase, and the Class a vehicle will require no increase in size.

The tradeoffs summarized in Table 5 that led to the RMEP drive-train point design are nominally valid for optimizing the MMR drive train. One more iteration of the same tradeoffs is recommended as part of a subsequent study. After determining environmental effects, the MMR drive motor selection will narrow to a choice between a permanent magnet brush motor (RMEP) and a D.C. Brushless Motor.

The magnetic materials considered suitable for the drive motor are samarium cobalt (preferred), platinum-cobalt, and alnico-9. They show the same general thermal characteristics. The following values are representative:

Magnet	% of 70°F Magnetic Properties		
	+70°F	+500°F	-200°F
Samarium-Cobalt <sup>(1)</sup>	100	94	103
Platinum-Cobalt <sup>(2)</sup>	100	75	102
Alnico 9 <sup>(3)</sup>	100	96	101

(1) Raytheon Co.

(2) Johnson Matthey and Co., Ltd.

(3) Thomas and Skinner Bulletin M304-C

**TABLE 5 RMEP DRIVE MOTOR-GEARBOX**

**SUMMARY OF CANDIDATES AND PARAMETERS**

**MOTOR**

D-C, BRUSH, PERMANENT MAGNET  
D-C, BRUSHLESS  
D-C, BRUSH, WOUND FIELD  
A-C, 400 HZ, HYSTERESIS SYNCHRONOUS  
A-C, 400 HZ, INDUCTION

SELECTED. SMALLEST – 5 IN.<sup>3</sup>  
LIGHTEST – 11 OZ

OFFERS HIGHEST COMBINED MOTOR –  
GEARBOX-CONTROLLER EFFICIENCY, 55%

**GEARBOX**

PLANETARY TYPE, 2 13/16 IN DIAM – EXCEEDS 1½ IN DIAM CONSTRAINT  
1 1/2 IN DIAM SELECTED, 8 OZ, 5 IN<sup>3</sup>, 7 FT-LB CONTIN., 94% EFF  
1 1/4 IN. DIAM – MAX TORQUE (2 FT-LB) INADEQUATE

**SELECTED DRIVE MOTOR-GEARBOX, POINT DESIGN SUMMARY**

D-C BRUSH, PERMANENT MAGNET/PLANETARY GEARBOX  
1½ IN. DIAM X 5.9 IN  
1.2 LB (19 OZ)  
28 VDC  
290/1 GEAR RATIO

NORMAL SPEED = 20 RPM = 1 MPH  
SPRINT SPEED = 40 RPM = 2 MPH  
LEVEL DRIVING (7 FT-LB) EFF = 58%  
SLOPE CLIMBING (14 FT-LB) EFF = 52%  
STALL TORQUE = 32 FT-LB

A modified RMEP planetary gear box appears to be adequate for the MMR applications. Environmental (cold temperature, low pressure) effects should be investigated during a subsequent study. Techniques utilized for Lunar Rover and Viking equipment should be extracted where appropriate.

During same subsequent study a "straw model" mobility subsystem cascaded to the electrical power supply will be configured using readily available components that can be modified to qualify for the Mars environment. An option will then exist for finalizing this design (adequate performance/low cost) or for further performance (minimum weight/volume) optimization via parametric analysis.

Subsystem optimization would tradeoff component types (constrained to nominally equal performance) against associated net weight and volume (including the power supply). Once selected, these component types can be further optimized in terms of the sensitivity of their weights and volumes to characteristics such as materials, applied voltage, etc. Parametric curves would then be generated to enable the selection of MMR designs that deviate from the straw model design.

Table 6 shows the RMEP wheel drive growth potential with relation to the selected point design. All three classes of MMR vehicles fall within the RMEP baseline design/power capability. The more powerful wheel drives will be held in abeyance for possible future interest.

#### 4.1 CONTROL CONFIGURATION

As for the RMEP, both open loop and closed loop mobility controls were considered. Since precise navigation is not required, both throttle and steering controls can be open loop, per the RMEP. This approach minimizes on-board complexity, weight, volume, and cost.

Vehicle control is implemented as follows. Assume that a remote operator by means of examining the facsimile camera's picture has determined a steer angle increment ( $\Delta \theta$ ) and a leg of travel increment ( $\Delta \ell$ ). Both these values are set into a control station console where they are encoded and sequentially transmitted to the vehicle.

TABLE 6 RMEP WHEEL DRIVE GROWTH POTENTIAL

WHEEL OUTPUT			VEHICLE WEIGHT, LB	MOTOR-GEARBOX			GEAR BOX	
TORQUE, LB-FT	SPEED, MPH	POWER, WATTS		WEIGHT, OZ	VOLUME, CU IN.	MOTOR DIAM, IN.	DIAM, IN.	RATIO
7	1	20	20	19	10.4	1½ (POINT DESIGN)	1½	290:1
10.8	0.65	20	31	33	20	1½	2.8	445:1
14	0.5	20	40	35	20	1½	2.8	580:1
7	2.65	53	20	64	32	2½	3	143:1
14	1.32	53	40	67	32	2½	3	286:1
21	0.88	53	60	70	32	2½	3	429:1

The steering command is the first to be processed. Steering is accomplished prior to each leg of travel by solenoid declutching one drive wheel from the motor drive assembly, and pivoting in either direction about the declutched wheel.

To start the steering sequence a digital number proportional to the wheel revolutions required to pivot through any angle between 0 and 360 degrees (in 10 degrees increments) is transmitted to the vehicle. It is addressed, decoded, and entered into a shift register. Next, the "STEER" command is transmitted which activates a clutching solenoid. A time delay later, the "GO" switch is automatically turned on and the unclutched wheel is driven. Its revolutions are sensed by a LED-photo transistor circuit which emits a pulse whenever an axle-mounted perforated disc interrupts the LED beam. These pulses are then counted in a digital counter. When the counter pulses are equivalent to the commanded steering angle in the shift register, a null is sensed which keys the drive motor switch off. A time delay later, the solenoid latch switch is automatically turned off, thus completing the steering sequence. (If dust is determined to be a problem for the LED-Phototransistor device, magnetic techniques can be used.)

The time delays permit declutching only when the drive train is stationary and ensure that the vehicle is "STOPPED" prior to the clutching actuation. The vehicle is now ready to execute a command to accomplish the incremental leg of travel ( $\Delta \ell$ ).

Operation is in many ways similar to steering. The desired value of  $\Delta \ell$  is entered into the shift register. A "GO" command is then transmitted. When  $\Delta \ell$  is accomplished a null is detected and the vehicle's drive motor automatically shuts off.

#### 4.2 DEPLOYMENT & ERECTION

The RMEP Deployment and Erection Scheme is illustrated in Figures 18 → 21. The possible adaption of this technique to the MMR is discussed in the section on "Environmental Effects." The less dense Martian atmosphere and lower gravity is accounted for in the discussion.

ORIGINAL PAGE IS  
OF POOR QUALITY

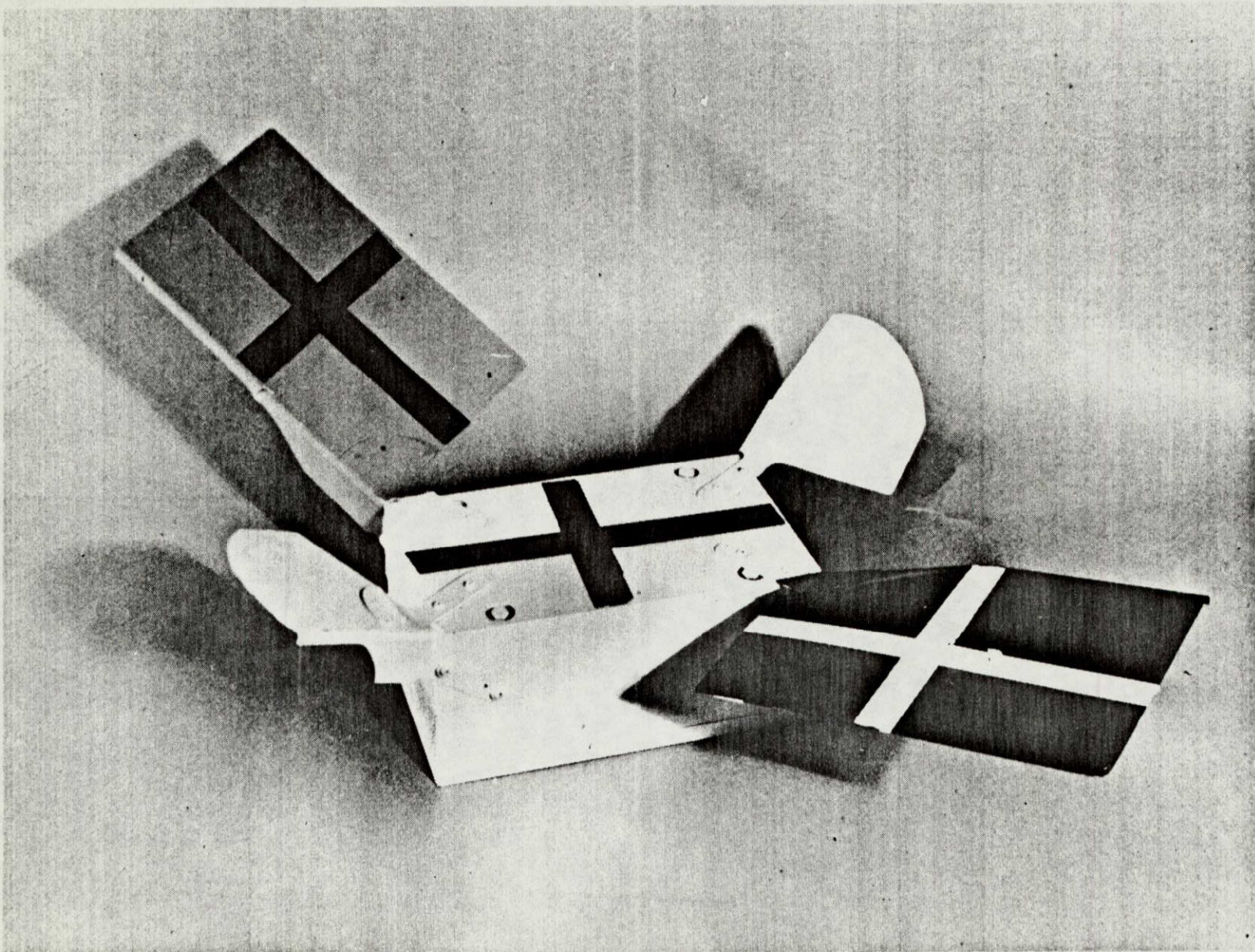


Fig. 18 Remote Mobile Emplacement Package-Stowed

ERECTION & DEPLOYMENT SEQUENCE

MINUTES:SECONDS

1. IMPACT SWITCH STARTS SEQUENCE		00:00
2. WHEEL MOTOR ROTATES 80° UNLOCKS AXLE		00:15
3. COMPRESSED AIR EXTENDS AXLES		00:15+
4. PUMP STARTS TO INFLATE WHEELS		00:15+
5. PUMP STOPS	TO LEVEL VEHICLE OR	06:21
6. WHEEL MOTOR REVERSES	ROTATE AXLE 200°	06:21
7. TAIL BOOM STACER EXTENDS		06:21+
8. WHEEL MOTOR FWD 280°/80° AFTER LEVEL		06:27
9. SOLAR ARRAY PANEL SWINGS OPEN		06:27+
10. MAST STARTS TO ROTATE UP FROM STOW		06:27+
11. SYSTEM SWITCHES FROM AUTO TO CMD		06:27+
12. MAST MOUNT ROTATES 90° AFT		06:29
13. MAST STACER EXTENDS CAMERA		06:29+
14. MAST STOPS IN VERTICAL POSITION		06:29+

2504-025

Fig. 19 Erection & Deployment Time Sequence

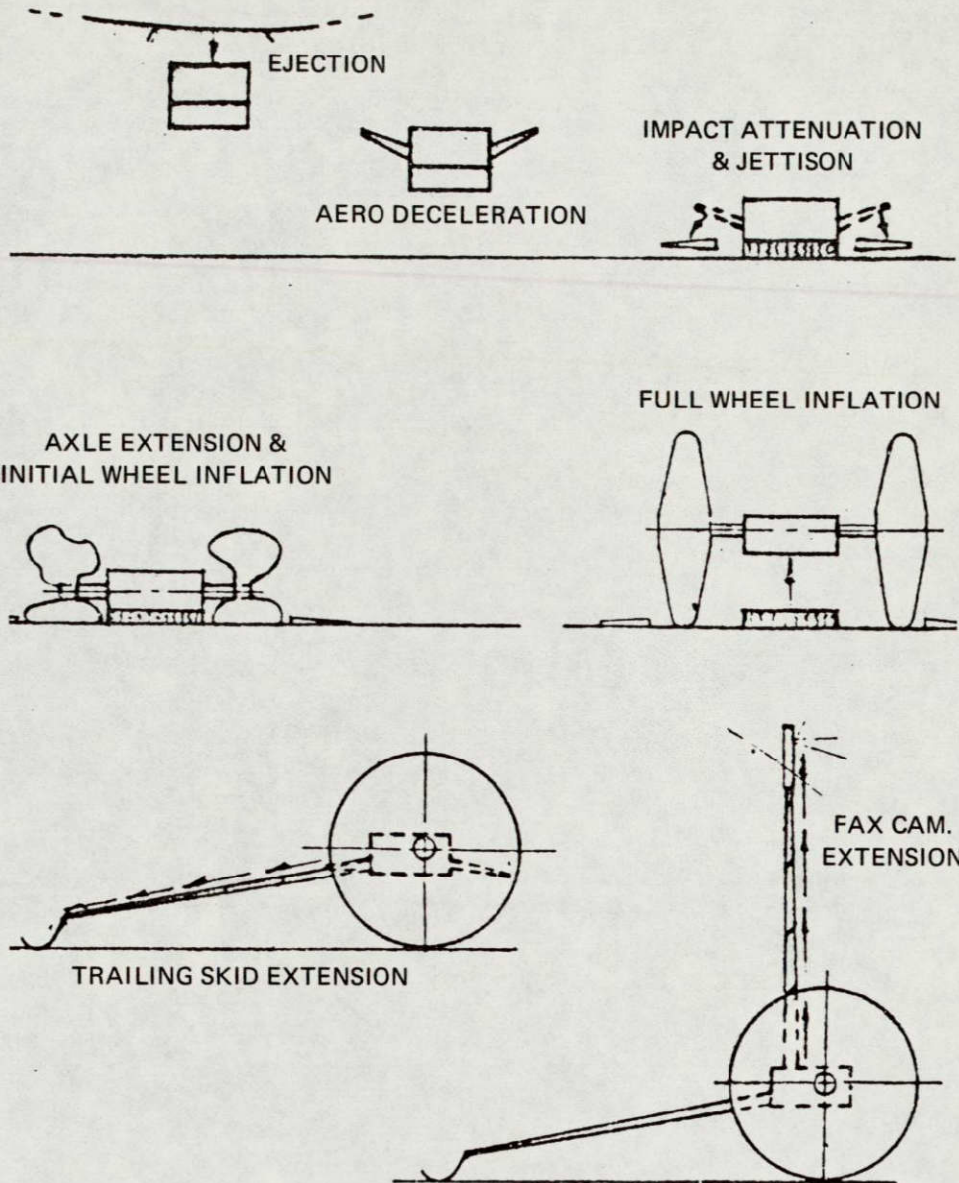


Fig. 20 Sequence of Emplacement Operation

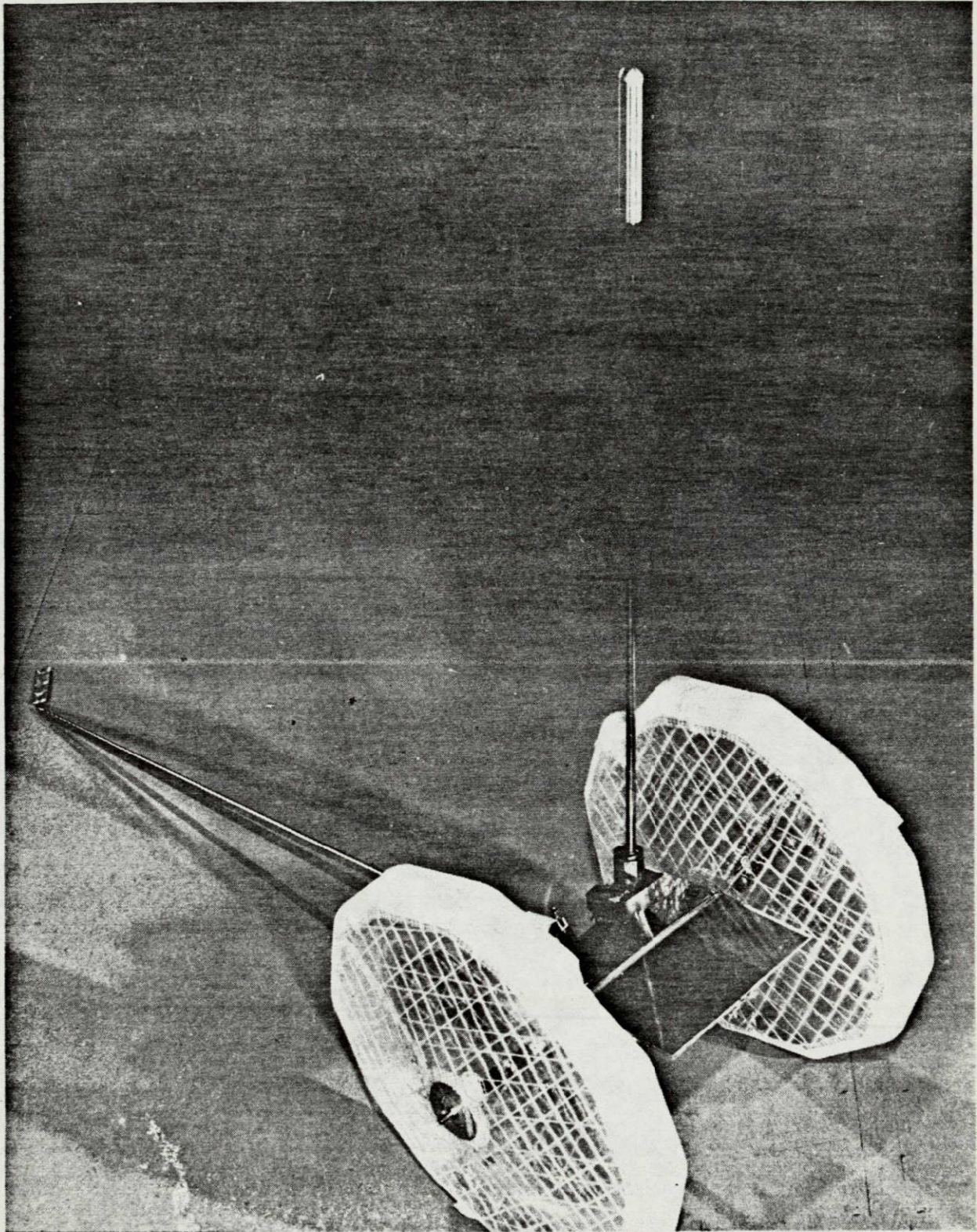


Fig. 21 Camera Mast Fully Extended

## 5.2 GROUND SLOPE & OBSTACLES

The nominal mean ground slope,  $\bar{S}$ , expected over the length of the rover, 1 m, is about 3°. For horizontal distances longer than the rover length,  $\bar{S}$  is less (i. e., 2° for 10 m and 1.5° for 100 m). The fraction, F, of the surface slopes exceeding any value S for a given  $\bar{S}$  is:

$$F = e^{-S/\bar{S}}$$

For  $\bar{S} = 3^\circ$  and  $S = 10^\circ$ , the fraction is 0.036, which is considered negligible. For values of S much larger than 10° the problem becomes that of climbing obstacles. Since the Martian slopes are generally less than those of the earth and "g" is less than that of the earth, no further electrical battery considerations for hill climbing are necessary at this time (see Table 3).

It appears, however, from the data we have that there are more obstacles on Mars than the terrestrial rover's power supply was designed for. For example, there could be one block larger than 20 cm in every square meter, and one block larger than 40 cm in every 10 m<sup>2</sup>. The effect of these blocks on the power supply requirements is yet to be determined.

## 5.3 ULTRAVIOLET RADIATION

It is well known that most plastics are seriously degraded by ultraviolet (UV) radiation. Of primary importance to the Mars mission is the effect of the uv radiation on the plastic inflatable wheels used on the rover. The present wheel material is a Mylar-Saran-Mylar<sup>TM</sup> laminate reinforced with Dacron<sup>TM</sup>. According to the Schjeldahl Company which manufactured the wheel, a protective coating of Hypalon<sup>TM</sup> or urethane may have to be used. This may increase the wheel weight by 45 percent, as well as the wheel stowed volume. The packing density of this heavier wheel and the effect of its weight and flexibility on the electrical requirements for functions such as hill and obstacle climbing and rolling resistance will have to be determined.

## 5.4 TEMPERATURE

There are two areas where the effect of the extreme cold (-100°C) operating temperature will have to be determined. The first is in connection with the lubrication of the motor, gears, bearings, etc. A dry lubricant, possibly Teflon<sup>R</sup>, in

enclosed areas, and Teflon<sup>R</sup> bearings in open areas may have to be considered as a solution to this problem. The effects of such a lubricant, and others, on the drive train efficiency will have to be found.

The second area involves the flexibility of the plastics used in the construction of the wheel. Polyester elastomers such as Mylar<sup>R</sup> and Hytrel<sup>TM</sup> possess mechanical properties such as flex-fatigue resistance, flexibility at low temperatures, resistances to deformation under moderate strain, and good abrasion resistance, which are important to the reliability and survivability of the MMR inflatable wheel. However, these properties are degraded at low temperatures where the materials can exhibit excessive brittleness. Plastics' handbooks state a brittleness temperature no lower than about  $-73^{\circ}\text{C}$  ( $-100^{\circ}\text{F}$ ) for these materials. As a result, if the MMR wheel is required to operate at temperatures lower than  $-73^{\circ}\text{C}$ , some heat will have to be supplied to the elastomers, possibly from a button RTG heater in each wheel hub. The power requirements of the RTG will have to be determined at a future time when the wheel size and shape are finalized. At the present time, the critical (low) temperature at which an unheated wheel can operate is to be considered close to  $-73^{\circ}\text{C}$ .

The goal of the present wheel design was to make 50 to 60 inflation-deflation cycles at  $-45^{\circ}\text{C}$  at an inflation pressure of 2 psi. If the inflation pressure is reduced to  $\frac{1}{2}$  psi, the wheel could probably cycle 500 times at a temperature of  $-55^{\circ}\text{C}$ . Moreover, if the material thickness is increased from 0.25 to 0.5 mil, we would probably observe an increased number of cycles to about 1.3 of the previous. The thicker material limits the minimum bend radius. The problem associated with wheel flexing is the formation of three-corner creases where pin holes are most likely to occur, especially at low temperatures. By constructing the wheel of many thin layers with an elastic adhesive in between, the survivability can be increased. In this case the failure of a single layer is not disastrous.

Of concern also is whether a "stiff" plastic wheel will require a larger internal pressure for proper erection at night in these cold temperatures. Since the tires will be inflated by a motor-driven pump, the electrical power requirements for each inflation-deflation cycle may change upward.

Schjeldahl has had significant experience with 0.5 mil Mylar<sup>R</sup> laminates operated at  $-195^{\circ}\text{C}$ . In this application, where there was no stress or  $\Delta P$  across the

material, they experienced over 100 cycles of operation. At a temperature of  $-55^{\circ}\text{C}$ , they obtained over 500 cycles. It appears that the MMR wheel can survive at very low temperatures,  $150^{\circ}\text{K}$  ( $-123^{\circ}\text{C}$ ), and have high operational reliability by controlling its low temperature exposure with an RTG.

There are several processes by which the wheels may be heated to allow for full operation at temperatures as low as  $-100^{\circ}\text{C}$ . These range from the conduction and convection of heat from a warm axle to such as the application of:

1. A resistance paint to the inner or outer surface of the wheel
2. A conducting strip or tape on one of the Mylar<sup>R</sup> laminations
3. A interwoven resistance wire or film sandwiched between laminations
4. A flexible resistance polyester layer in place of one of the structural laminations
5. A combination of the above, all electrically powered.

Materials for four (4) already have been designed by the LBJ Space Center and may be the most reliable approach to take. Use of this material permits pin holes and tears to occur in the heater material without complete loss of the heater and subsequently the wheel. Further study is needed in this area. In addition, it is anticipated that a test program for a heated wheel will be required.

#### Thermal Blanket

The equipment needed for both mobility and scientific operations falls into groups such as: electric motors, actuators, batteries, RTG's, electronics and others. In general, each group has its own maximum and minimum temperature limitations for either storage or operation as shown in Table 7. For example, CMOS and most other electronic components may be stored at  $-65^{\circ}\text{C}$  but can only operate reliably at  $-55^{\circ}\text{C}$ . Thus, it appears that electronic components necessary for mobility will have to be heated during the entire mission (i. e., while in transit as well as when on Mars). To minimize heater power it would be advantageous to have all electronic components including those necessary for science located in the same container.

The thermal stability of the heaters for the electronics and batteries is stated as  $\pm 10^{\circ}\text{C}$  in Table 7. In the case of the batteries, these are suggested tolerances from the manufacturers for optimum battery performance. For the electronics,

TABLE 7 THERMAL REQUIREMENTS OF COMPONENTS

GROUP	MINIMUM TEMPERATURE		HEATER		
	STORAGE	OPERATIONAL	REQUIRED	ACCURACY	POWER
MOTORS	NONE	OK ON MARS	NO	—	0
CMOS ELECTRONICS	-65°C	-55°C	YES	± 10°C	TBD
CCD's	TBD	-40°C	YES	—	TBD
ELECTRO-MAG ACTUATORS	NONE	OK ON MARS	NO	—	0
WHEELS	-195°C	-73°C	YES	± 10°C	TBD
NI-CD BATTERIES	-29 TO -40°C	0 TO 30°C	YES	± 10°C	TBD
LITHIUM BATTERIES	-40°C	-2 TO +27°C	YES	± 10°C	TBD
TETHER CANISTER	NONE	-73°C	YES	± 10°C	TBD
RTG's	MAXIMUM TEMPERATURE PROTECTION ONLY		NO	—	0

however, the accuracy stated is for minimum heater requirements (i.e., the colder a component operates, the less heater power is required), and it, therefore, is advisable to keep these components near their minimum acceptable temperature without heating to a higher temperature.

Since the heating load on an RTG will have short-time (thermostatic) variations as mentioned immediately above, as well as longer period variations (day-night or orbital vs operational), protective circuitry for the RTG heater power supply seems necessary to prevent elevated temperatures within the RTG. In addition to the variable heating demand associated with the mobility equipment, the payload equipment also will have a variable electrical heating demand.

With the assumption that on-board button RTG's will supply the heater power, the cross-sectional dimensions of the power line in the tether for the Class a and b vehicles will remain unchanged. However, RTG isolation (gamma rays and neutrons) may require radiation shielding for components on all vehicles.

It is impossible at this time to estimate the heater power requirements for each group listed in Table 7 until a point design is made, which will include the science packages as well. Then a study of the radiation and convection heat losses of the entire vehicle as well as the internal heat conduction through the structure can be made. At that time the form factor of the heater(s) can be made also.

## 5.5 WHEEL INFLATION PROCESS

The work required to inflate a wheel by pumping from a local atmosphere is given by:

$$W = V_w \left\{ (P_A + \Delta P) \ln \left[ \frac{(P_A + \Delta P)}{P_A} \right] - \Delta P \right\}$$

where  $W$  = work done,  $V_w$  = volume of wheel,  $P_A$  = ambient pressure, and  $\Delta P$  = wheel inflation pressure above the ambient pressure. For  $\Delta P = 3$  psi, the work done in the Mars atmosphere is 28 times that done in the Earth's atmosphere. However, by redesigning the wheel to reduce  $\Delta P$  to 0.5 psi the factor of 28 can be reduced to 2.2. Night time inflation of the wheel could reduce the factor to 1.1 at locations of extreme night and day temperature changes.

The phase diagram for carbon dioxide and water is shown in Figure 22. At the surface of Mars, shown at the upper left, the vapor pressure curve is at a temperature

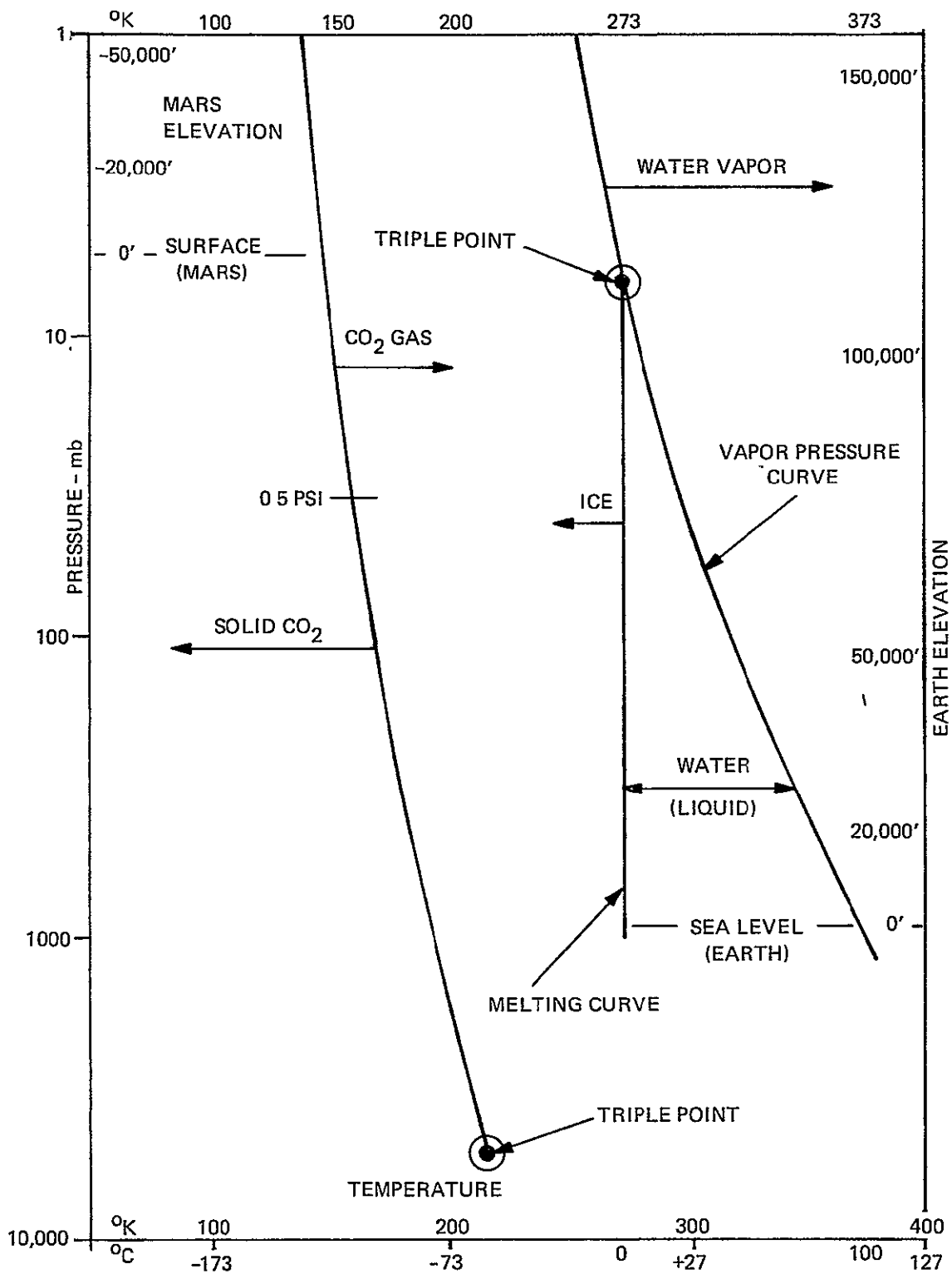


Fig 22 Phase Diagram For CO<sub>2</sub> and H<sub>2</sub>O

of only a few degrees below 150°K. At 180°K, where the MMR is required to operate, the vapor pressure curve is at 300 mb (4.4 psi). This curve points out the importance of not allowing the pressure within the pump during a compression cycle to rise much above the wheel inflation pressure of 0.5 psi (35 mb) to prevent the gaseous CO<sub>2</sub> from changing phase to the solid.

Some preliminary and rather simple calculations point toward a net value of 1.5 watt-minutes to inflate each 20-inch diameter wheel to 0.5 psi. This number will have to be increased by the cascade efficiencies of the motor and pump, the power required to unfold the wheel, the temperature of the gas, and other factors to be determined. A complete re-evaluation of the wheel design and landing site therefore has to be made before the electrical requirements for inflation can be evaluated accurately. At the same time, a Mars wheel inflation time can be calculated.

In addition to the work required to inflate a wheel, the inflation process also raises the entire vehicle off the soil. Since the Mars "g" is 0.38 of Earth "g", there will be some electrical savings during the raising process. It is not known at this time what fraction of the electrical budget is affected, but it is expected to be rather small.

To estimate accurately the work required to inflate a wheel, two additional parameters become important. One of these involves the compression process of the pump, i. e., isothermal, polytropic, or isentropic (adiabatic). Another is the gas involved, CO<sub>2</sub> for the Mars atmosphere vs O<sub>2</sub> and N<sub>2</sub> for the earth atmosphere. The variable of importance with these gases is the ratio of specific heats  $C_p/C_v$ ,  $\gamma$ . If the compression process is isothermal, both atmospheres will require the same work, independent of  $\gamma$ . If the compression process is isentropic, however, more work is required, as a function of  $\gamma$ . The larger  $\gamma$  (1.4) for the earth's atmosphere requires more work per compression cycle than the smaller  $\gamma$  (1.28) for the Mars atmosphere. The work required for the polytropic process lies between that of Earth and Mars and is the process expected on Mars.

Although the role of  $\gamma$  is well known when estimating the work required for a positive displacement compression cycle [of the form  $(\gamma/1 - \gamma) (P_2/P_1)^{(\gamma - 1)/\gamma - 1}$ ] it is yet to be determined if the same number of compression cycles are required to inflate an identical wheel for both the Earth and Mars atmospheres.

The leakage rate of the wheel when filled with air has been determined and found acceptable for the 20-inch diameter wheel. A parallel study or measurement will have to be made for a wheel inflated with CO<sub>2</sub> to determine the permeability of the plastic to CO<sub>2</sub>, and the resulting power requirements for re-inflation, if necessary.

#### 5.6 ROLLING RESISTANCE

The resistance of the rover wheels to the Mars soil will have a definite impact on the electrical budget. In general, a larger diameter wheel or a wider wheel will create less rolling resistance for a given vehicle weight. It appears, at this time, that a larger wheel will be required because of the obstacle size, which should have some reducing effect on the electrical budget, provided the volume and weight of the wheel are not overwhelming. A tradeoff analysis of the wheel parameters including the rolling resistance will have to be made to establish the overall effect.

#### 5.7 OUTGASSING

Some materials, especially plastics, exhibit outgassing when in a vacuum environment. Since the transit time from earth to Mars is about one year, and in a nearly perfect vacuum, the rate of outgassing of these materials is important from the point of view of venting the stored wheel while in transit. If trapped gas collects in the folded wheel during transit sufficiently to pressurize it and increase its stored volume, a problem may arise at the time the wheel is expelled from the wheel cup, either by damaging the wheel or by having the wheel bind in the cup.

After an initial period of 24 hours in a dry environment, most plastic materials are cataloged as having an outgassing rate close to  $10^{-7}$  Torr l/s.cm<sup>2</sup>. If the inner laminate of the wheel is Mylar<sup>®</sup>, which may possess such an outgassing rate, the wheel would become partially pressurized after a one year travel in space. To prevent this partial pressurization from occurring, it appears that each wheel will have to contain a vent during flight. The vent in turn would be used for the inflation as well as the deflation tube while on Mars.

#### 5.8 HARD LANDING (100-kg VEHICLE)

To control the terminal velocity of the terrestrial RMEP when dropped from aloft, a set of blades was attached to control the descent speed. The blades also were given a pitch so that the RMEP package would autorotate during its descent. Under

these conditions the terminal velocity was limited to about 17 m/s. In the Mars atmosphere,  $\rho = \rho_{\text{Earth}}/100$  and " $g$ " = 0.38 " $g_{\text{Earth}}$ ", the terminal velocity would be about  $17(38)^{1/2}$  m/s or about 105 m/s, other things being equal. Since this terminal velocity is rather large, the design of the blades would have to be changed; in particular, the blade disc area will have to be increased and the pitch of the blades will have to be re-examined. Tests of a 1/10 scale model will probably have to be made to verify the blade design. Further information on the RMEP blade design can be found in Reference G.

Another aspect still to be considered of the hard lander in free fall is its righting moment in the Mars atmosphere in the event the package is released at altitude either inverted or on its side.

## Section 6

### MMR RELIABILITY/SURVIVABILITY - GENERAL OBSERVATIONS

Figures 23 and 24 illustrate the MMR Class I and Class II mobility scenarios and serve to place the following discussions in perspective.

The tiny RMEP (10 x 6 x 4.8 inches stowed) weighing 20 pounds including facsimile camera, payload, and a full complement of subsystems contains mobility power capability in excess of both Class I and II MMR requirements - (see Table 8). This favorable mobility power comparison ( $\cong 8, \leq 30$ ) combined with the more relaxed MMR Class a and b vehicle weight allocations (44 and 110 pounds) enables the following considerations regarding increasing MMR reliability/survivability:

1. Consider replacing the RMEP's brushed D.C. permanent magnet motor with a more reliable brushless D.C. machine
2. Determine if the additional vehicle weight allowance permits elimination of the wheel drive gear box by implementing the brushless D.C. motor in a heavier/larger "torquer" configuration
- 3.- Consider providing sufficient on-board energy redundancy (and a communications subsystem) to accomplish a large part or all of the mission in the event of tether failure - or totally replacing the tethered RTG/Battery Class a and b Electrical Power Supply with an on-board primary battery and RF communications subsystem (refer to Table 8). The 44-pound Class a MMR requires 2.6 watt-hour of mobility energy to complete its 200 m sortie. Grumman has been "designing in" Lithium Thionyl Chloride primary batteries into other proprietary remote control vehicles. These batteries (depending on drain rates) can practically be expected to furnish  $\approx 200$  W-hr/lb and 17 W-hr/in.<sup>3</sup> - subject to adequate thermal management. The above 2.6 W-hr of mobility would require  $\approx 0.013$  lb of battery at a volume of  $\approx 0.15$  in.<sup>3</sup>. Ninety inflate-deflate cycles are estimated to require less than 90 W-hr total, which equates to a  $\Delta 0.45$  lb/ $\Delta 5.29$  in.<sup>3</sup> of battery.

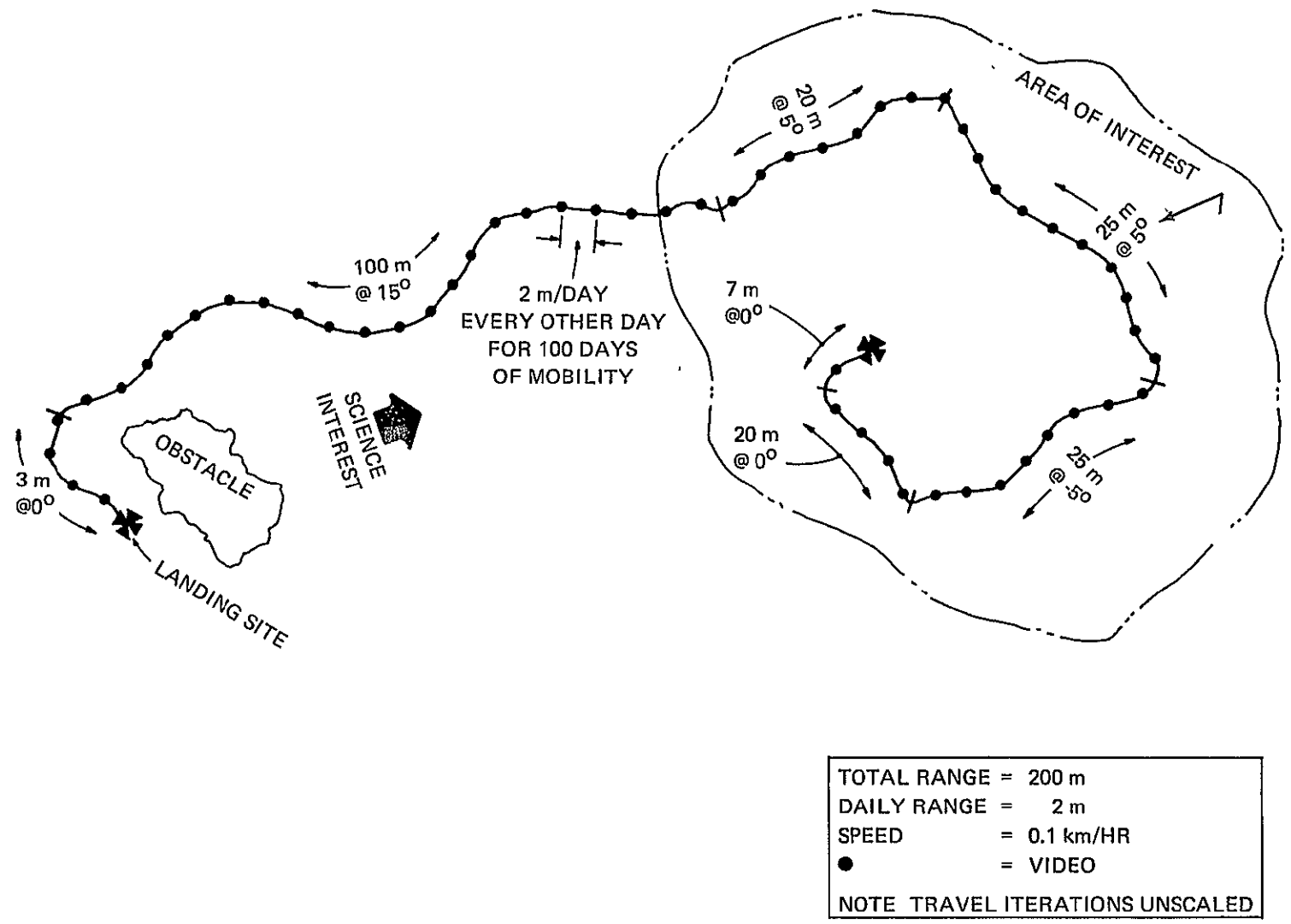


Fig. 23 Mars Mini Rover Class I Mission

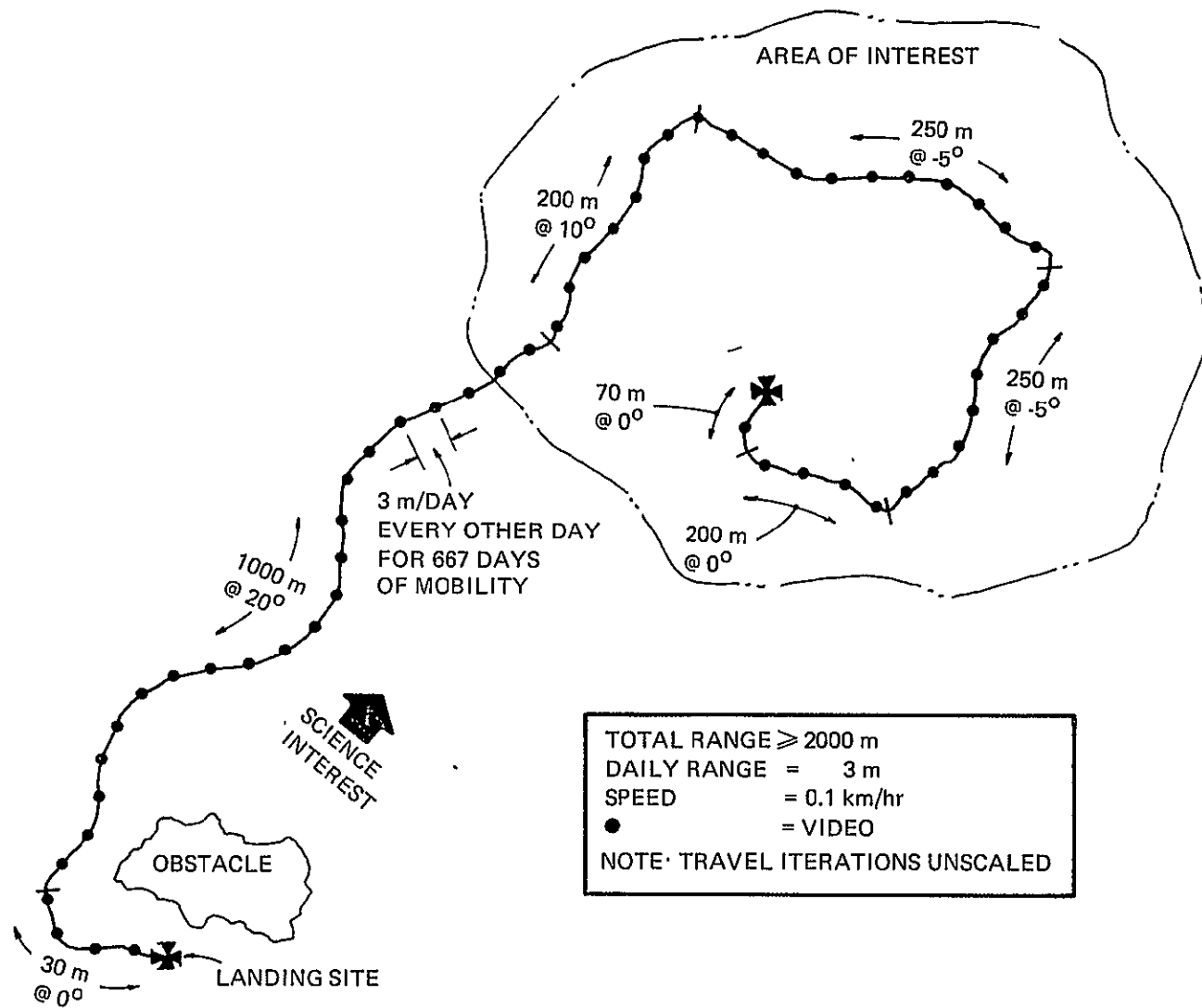


Figure 24 Mars Mini Rover Class II Mission

TABLE 8. RMEP/MMR RELATIVE MOBILITY DATA

	RMEP (EARTH APPLICATION)	CLASS I MISSION		CLASS II MISSION
		(a)	(b)	(c)
TOTAL ALLOCATED WEIGHT (LB)	20	44	110	220
PAYLOAD WEIGHT (LB)	INCLUDED IN ABOVE	13	35	57
BALANCE AVAILABLE FOR MMR	—	31	75	163
TOTAL VEHICLE TRACTIVE FORCE (LB)	8.4	5.58	10.8	20.23
WHEEL DIAMETER (IN.)	20	36	36	48
VEHICLE SPEED (KM/HR)	1.6	0.1	0.1	0.1
WHEEL RPM	20	0.59	0.59	0.44
TOTAL WHEEL TORQUE (FT-LB)	7	7.8	16.2	40.5
TOTAL OUTPUT WHEEL POWER (WATTS)	20	0.65	1.35	2.53
NOMINAL WATT-HOURS/KM ( $\eta = 50\%$ )	64.6	13	27	50.6

The 110-lb MMR would require 0.027 lb/0.32 in.<sup>3</sup> and 0.45 lb/5.29 in.<sup>3</sup> of battery for mobility and inflation-deflation respectively.

The above quantitatively demonstrates that the relatively small battery requirements for mobility and inflation-deflation cycles, in the context of the total allocated weight, open up some optimistic options - for extensive on-board energy redundancy in the event of tether failure - or elimination of the tether altogether for Class I missions. While the Class c MMR could also be battery powered - 0.5 lb/6 in.<sup>3</sup> and 13.6 lb/161 in.<sup>3</sup> for mobility and inflation-deflation, respectively, it may be more practical to use the on-board RTG as planned. The more relaxed Class c weight allocation (in comparison with the RMEP) will enable a conservative vehicle design. In any event, all MMR vehicles can at least be designed with a substantially redundant energy supply. Payload power/duty cycles are yet to be factored in.

4. No vehicle brakes will be required for Class a and b MMR's as braking is inherent via the gear ratio. Class c braking characteristics are to be determined.
5. At this point, it is possible (subject to further study) that by adhering to RMEP packing densities in the MMR design, two Class a or b MMR's might be delivered in the place of one - with a modest increase in the 44 pound weight constraint. Volume allocations are as yet to be furnished to Grumman. The Class c MMR should be further studied to also determine if two MMR's can fit within the 220 pound weight allocation. If the Probability of Success ( $R_1$ ) of one MMR is 0.9 for example, two totally redundant MMR's would improve the Probability of Success to  $R_2 = 0.99$ .
6. Future study should determine if it is possible and practical to inject a foam into the MMR wheels under emergency leakage conditions (beyond the practical limit of pump replenishment). The wheels will then be permanently "inflated" and a "standby" mechanical screw jack would be employed to move sleeves covering two universal joints that are contained in the axle. The latter would enable the payload to mechanically "touch down" on the ground (and back up again) as during the deflate maneuver.

## MMR SYSTEM OPTIMIZATION

While it has been shown that the RMEP adaption to the MMR is feasible and practical, an optimized configuration design is yet to be performed. For this to be accomplished the stowed volume and form-factors for fitting the MMR into the delivery vehicle and for fitting the science payload into the MMR, must be provided. Grumman has a wide variety of previous Remote Control Vehicle designs that should be considered prior to freezing the MMR design. Figure 2 illustrates a scale model of one of these designs undergoing obstacle negotiation tests. Noteworthy is the fact that this configuration can climb positive obstacles equal to the vehicle's wheel diameter.

## Section 7

### CONCLUSIONS AND RECOMMENDATIONS

Based on this limited "Phase O" feasibility study, it was found that the RMEP designed as an Earth rover, has application for use as an MMR during the post 84 Mars missions, provided that reasonable modifications identified in this report are made. These conclusions were obtained by considering References E and F, and by the application of prerequisite requirements and constraints data supplied by JPL.

The applicability of the RMEP design concept and specific subsystems as candidates for the Mars missions was extrapolated with respect to: deployment, mobility, control-navigation, communications, hazard detection and avoidance, and energy management. Emphasis was given to the wheel subsystem. Modifications to the basic wheel design are required primarily due to environmental constraints. These modifications involve: protection of plastics from uv radiation, wheel tread improvements, wheel side loading (structural) resistance, and low temperature operation. Increases in MMR payload and obstacle clearance over the RMEP design present no fundamental problems. Several parameters, however, remain to be determined such as: total electrical demand, thermal blanket form factor, reverse direction routine, and tether payout device details.

Another study at a Phase B level is recommended to further analyze and synthesize the wheel design and to reduce the uncertainty in the vehicle(s) sizes, weights, and thermal requirements as well as to converge on the final methods for mobility, control-navigation, and hazard detection and avoidance.

## Section 8

### ESTIMATED COST TO CONTINUE DEVELOPMENT OF THE RMEP

It is beyond both the technical and financial scope of a "Phase O" effort to estimate the costs necessary to modify the RMEP for a Mars application. However, Grumman has previously estimated the cost of a "Phase III" RMEP which called for designing the vehicle to survive a 1,000 g impact airdrop, integration of a GFE communications subsystem and facsimile camera, design and development of an integral power supply, further miniaturization of the vehicle's electronics and fabrication of a complete vehicle to demonstrate mission capability. Control of the vehicle during the demonstrations would be through a ground station data link where facsimile camera images could be used to command vehicle movements. Study and evaluation of a hazard warning system was also to be included. Completion of this "Phase III" would take approximately 14 months and cost approximately \$1,124,000 (including fixed fee).

## Section 9

### NEW TECHNOLOGY

No reportable items of new technology have been identified.

## REFERENCES

- A. NASA Technical Note, TN D-7462, A Conceptual Design and Operational Characteristics for a Mars Rover for a 1979 or 1981 Viking Science Mission, February 1974.
- B. JPL Interoffice Memo, 3577-77-06, Preliminary Mars Surface Environmental Estimates for Mars Rover, 1 February 1977.
- C. Bekker, M. G., Off-The-Road Locomotion, University of Michigan Press, 1960.
- D. G. T. Schjeldahl Co., Inflatable Toroidal Wheel, GAC PO 0-16230, 30 July 1971.
- E. Remote Mobile Emplacement System (U), Feasibility Study, Final Report, Grumman Aerospace Corp., GR-00-35, 591-I70, August 1970 (Secret).
- F. Remote Mobile Emplacement System (U), Phase II, Final Report, Grumman Aerospace Corp., GR-00-40, 498-I71, October 1971 (Secret).
- G. Wohllebe, F., Summary of Calculated and Experimental Results of an Auto-rotating Package for Special Projects, Grumman Aerospace Corp., AERDYN-Memo/71-24, 1 November 1971.
- H. Dual Mode Lunar Roving Vehicle - Preliminary Design Study, Grumman Aerospace Corp., January 1970, NAS8-25098.
- I. Hazard Detection Methods for a Lunar Roving Vehicle, Grumman Aerospace Corp., January 1970, NAS8-25098.
- J. Hazard Detection and Avoidance System for a Lunar Roving Vehicle, July 1970, Grumman ADR 06-04-70.2.

## Appendix

### SURFACE HAZARD DETECTION

#### OPTICAL SYSTEM

General - The space, weight and power guidelines set down for a hazard detection system for the LRV have limited the investigation of optical sensing systems to small low power devices such as electroluminescent diodes and lasers. A bumper made up of electroluminescent diodes appears to be the smallest and lowest power device that could be used for obstacle detection. However, its relatively large beamwidth compared to standard lasers would introduce large amounts of background noise due to reflected sunlight. Thus, under the variety of lighting conditions expected on the lunar surface, the return from an electroluminescent diode could only be detected through coding of the signal and complex signal analysis. Since a lasing diode can be used with a small sacrifice in power, the study was concentrated on lasers.

In the past decade research and development on lasers has produced devices to fill the needs in many technological fields. Many of the applications are high powered devices. In addition, a low power, solid-state, injection laser has been developed - the Gallium Arsenide (Ga As) diode. The Ga As diode has been used in systems capable of detecting targets at ranges from three feet to several thousand feet.

The range requirements for obstacle detection for the LRV are dictated by the vehicle stopping distance of 1 meter in the unmanned mode to eight meters in the manned mode. The following analysis indicates the advantage that a Ga As laser system has in meeting the low power requirements of the hazard detection system.

Investigation of Laser Techniques - The laser pulse power needed to overcome the lunar background determines a large part of the power needed. The background power can be calculated from:

$$P_b = M \cdot \Omega_r \cdot A_r \cdot \Delta\lambda \cdot T_r \cdot \rho \cdot \pi^{-1}$$

where M is the spectral solar irradiance ( $0.85 \text{ W}/\mu\text{cm}^2$ ) in IR range),  $\Omega_r$  is the beam divergence of the receiver (in steradians),  $A_r$  is the area of the receiving

aperture,  $\Delta \lambda$  is the spectral bandwidth,  $T_r$  is the transmission of the receiver optics, and  $\rho$  is the reflectivity of the lunar surface.

In the typical case of short range detection the receiver may have a  $1^\circ$  or approximately  $2.5 \times 10^{-4}$  steradian field and an area of  $5 \text{ cm}^2$  (these vary with the system chosen). A  $100 \text{ \AA}$  ( $10^{-2} \mu$ ) bandwidth filter is used to minimize background and  $T_r = 0.5$  is typical for the transmission of the optics. The reflectivity of the moon is taken as 0.1 in the near IR. This results in a received background power of  $1.7 \times 10^{-8} \text{ W}$ . For long-range detection the receiver field would be smaller and thus received background power would be lower.

The received signal power can be calculated using:

$$P_s = P_o \cdot A_r \cdot \rho \cdot T_r \cdot T_t / R^2$$

where  $P_o$  is the peak laser power,  $T_t$  is the transmission of the laser optics and  $R$  is the range being measured. With  $T_t = 0.9$  for the transmitter optics and  $R = 2 \text{ m}$  (200 cm) the received signal power is  $1.8 \times 10^{-6} P_o$ . For  $R = 10 \text{ m}$  ( $10^3 \text{ cm}$ ) the received signal power is  $7 \times 10^{-8} P_o$ . The retroreflective nature of the lunar surface would increase these factors. State-of-the-art laser diodes can provide sufficient peak power (5 to 11 W) so that the received power would be much greater than the background power. With 100 nsec pulses at 1000 pps a typical duty factor would be  $10^{-4}$ . Thus, even if the efficiency of the laser is as low as 0.1 percent, less than a watt of average power will be consumed by it and its pulser.

There are basically three ways that terrain obstacles can be detected with laser techniques: direct ranging, loss of return by interruption of beam path, or return from obstacles.

Ranging to detect obstacles basically consists of scanning the area in front of the vehicle and recording the range to each point as the laser fires. In this way a grid of ranges is established. From the geometry of the vehicle and laser the "expected" range results for each point are known in advance. Thus the obstacle detection involves the correlation of "obtained" versus "expected" range in order to find range anomalies due to holes, rocks, slopes, etc. ITT is working on modifying their laser docking device\* to accomplish this. The device consists of a piezoelectrically

-----  
 \*Dixon, T., Cardone, L, Flom, T., Laser Guidance System, Brochure No. 0429, prepared by ITT Aerospace, Optical Div., San Fernando, Calif, 1969.

scanned Ga As laser and an image dissector. Reported accuracy with the device is equal to 10 cm from 1 to 20 m using 10 W total. However, in this system the correlation function is separate (not part of the 10 W) and involves enormous data handling in that each point must be stored and compared with a standard or the next set of points. Even at low laser pulse rates the data builds up quickly, resulting in complex data processing. While this method gives a very detailed map of the terrain, a system which does not require sophisticated data handling is desirable if adequate range and resolution can be obtained.

The other two methods, "loss of return by interruption of beam path," or "return from obstacles," are basically the same. In both cases the laser and receiver are positioned to allow the laser beam to hit the receiver only when no obstacles are present in the first case or only when one is present in the second case. The best example of these approaches is the "laser cane".\* In these methods no complex ranging or correlation is required as they intrinsically range and detect obstacles.

The major portion of the optical hazard detection study was devoted to an analysis of the principle of the laser cane. In this approach the laser beam and receiver field of view intersect at ground level. If the laser beam hits a certain amount above or below this point of intercept none of it is reflected into the receiver. A diagram of this concept is shown in Figure 25.

As shown in Figure 25, the laser might be mounted on the LRV mast and the receiver about 50 cm below it. The laser beam will be detected by the narrow field of view receiver only if it hits within the target detection area defined by the beam and the limits of the receiver field of view. Thus any obstacle (hole or boulder) which causes the beam to hit outside this area will result in the receiver not picking up the laser return.

It has been shown previously that a Ga As laser system can meet the long and short range detection requirements well within the guideline power constraints. The resolution will be a function of the laser beamwidth and the width of the limited field

-----  
\*The Design Manufacture and Laboratory Testing of the Veterans Administration's Obstacle Detection Model G-5, Bionic Instruments, Inc., Bala Cynwyd, Pa., December 1963.

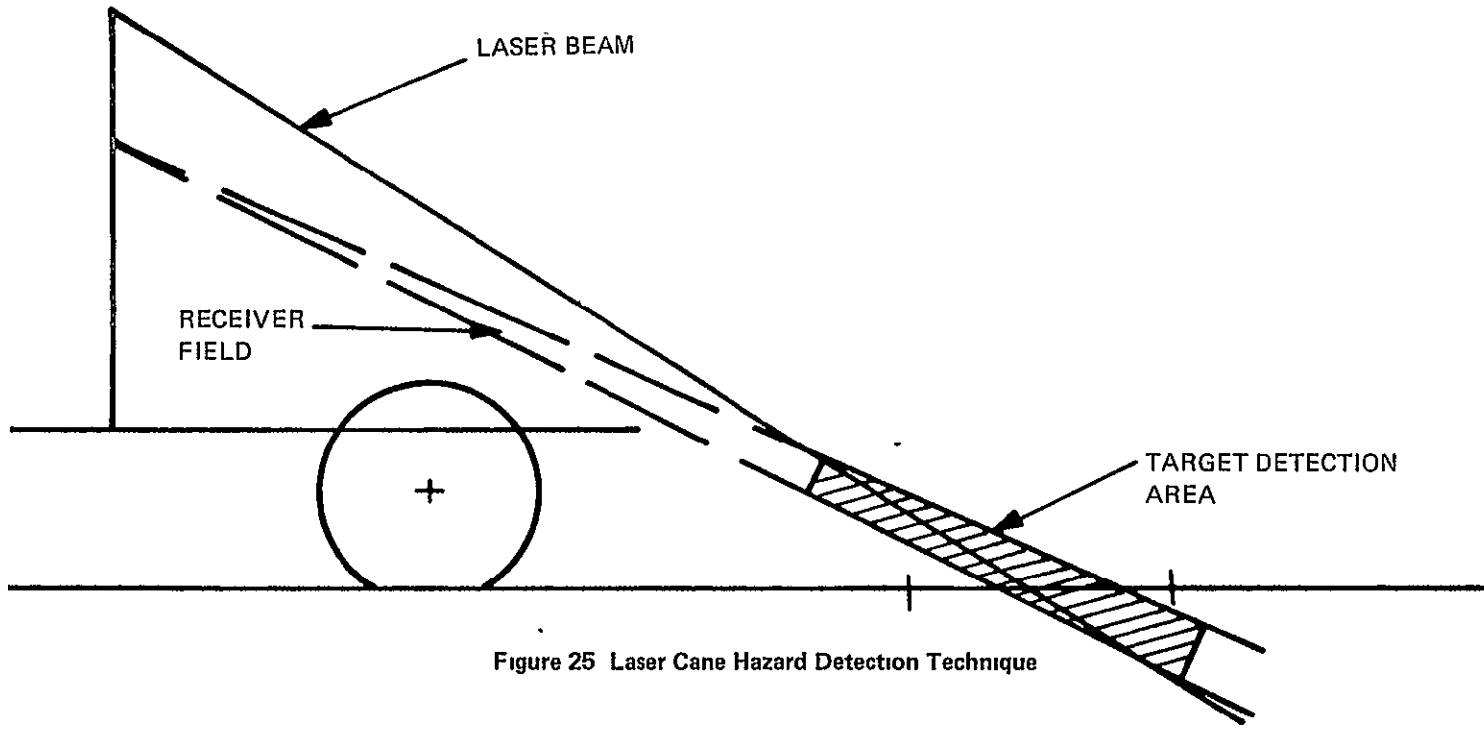


Figure 25 Laser Cane Hazard Detection Technique

of view receiver. For example, the angular resolution needed to discern differences of 10 cm at 10 m range is on the order of half a degree. This order of collimation is readily attainable with a simple lens collimator. The narrow field of view receiver is also readily attainable with baffles or apertures.

An area of major concern in an optical detection system or in any direct viewing system is the line of sight problem. With the sensor mounted at a reasonable height, the ability to discern the depths of holes is difficult. The reasons for this is that for a typical 1-m obstacle the laser beam will enter a hole and hit the far side before it hits the depth of the hole but on its width.

As an example of this, at 10 m the angle between the ground and laser beam is about 10 deg. This results in a drop of 15 cm by the beam as it traverses a 1-m-wide hole (potential minimum obstacle). Thus, if the laser cane is designed to detect hole widths as small as 1 m, the detected holes may only be 15 cm deep, which is not an obstacle. This results in a range of depths for holes which are falsely registered as obstacles. The range of false alarms is illustrated in Figure 26, which shows a no-return (obstacle) condition. The maximum depth of an undetected hole may be increased but only by enlarging the minimum width of the holes to be detected or by increasing the angle between the laser beam and ground.

This problem has been recognized by all personnel involved with hazard detection including LRV project and NASA personnel. The present philosophy is that in long-range detection, which is a necessary requirement in the high-speed mode, the detection of the top of the hole is sufficient. This detection would signal a slow mode command to the vehicle and determination of the depth of the hole would wait until a closer observation could be made.

Up to this point the discussion has evolved around the capability of the optical system to detect targets in a single vertical plane. Since the LRV has a proposed width of approximately 112 inches, the detection system must provide an azimuth coverage somewhat greater than this to assure that all obstacles in its path can be detected.

The azimuth coverage can readily be provided by an array of lasers and detectors or by scanning techniques. Low power scanning devices are available using piezoelectric or torsional techniques.

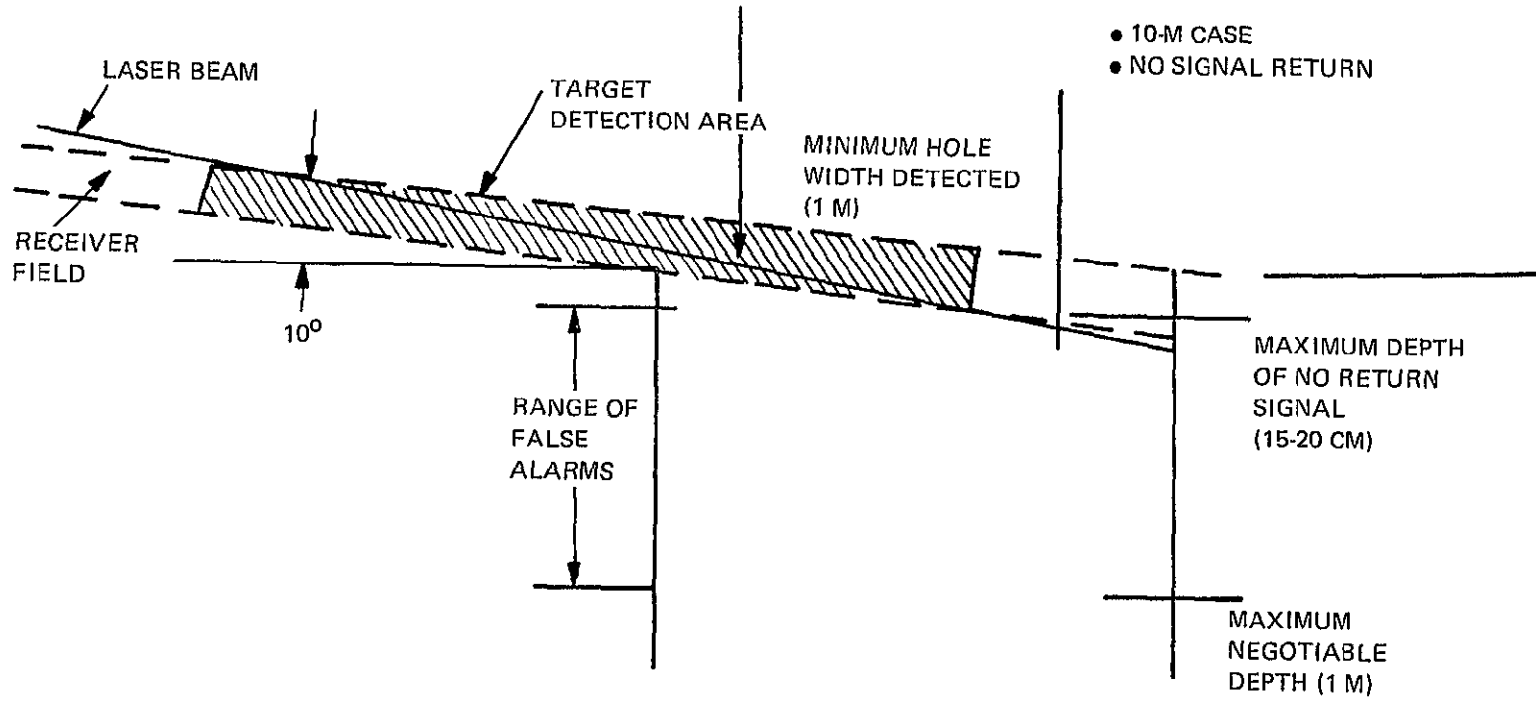


Figure 26 Laser Cane Hole Detection

A piezoelectric scanner uses a mirror mounted on a crystal. When high electric fields are applied to the crystal its planar orientation changes causing deflection of the mirror. Strain gauges and feedback loops regulate the deflection of the crystal.

Small angular deflections are obtained by this method and enlarged by the use of negative lenses. IIT employs such a scanner in their laser docking device.

Torsional scanners consist of a mirror attached to a taut band. Magnetic material is attached to the back of the mirror which is mounted with two electromagnets behind it. By pulsing the electromagnets the mirror-band system can be driven as a torsional pendulum near its resonant frequency. These devices have obtained up to  $10^\circ$  deflection at 100 cps using less than a watt of power.

A further alternative to the use of detector arrays or scanning is the use of an image dissector as the receiver. In an image dissector the photon image creates an electron image at the photo cathode. This electron image is deflected and sampled by an aperture and fed to a photomultiplier dynode structure allowing low light level detection. In this technique the scanning laser is followed by the image dissector which completes the laser cane loop. In this manner the required azimuthal coverage could be obtained.

In all cases the forward motion of the vehicle provides the other dimension of scan so that the detector sweeps the area as it enters it. Alternately two dimensional scanning could be used at the cost of complexity, reliability, and power.

Another major concern for hazard detection is the detection of slopes. Sharp slopes will appear as positive or negative obstacles before the vehicle is on them. The closer a vehicle gets to a sharp slope the more that slope will resemble an obstacle. For example, in one meter a  $35^\circ$  slope will rise 70 cm. Thus, if a laser cane detects one meter in front of the vehicle a  $35^\circ$  slope will appear as a 70-cm obstacle as the vehicle is about to start up the slope. Therefore, the maximum negotiable slope must be considered in determining the obstacle threshold.

The "laser cane" device is essentially a go-no-go technique. Actual size of obstacles cannot be determined. Their occurrence can only be detected if they are large enough to interrupt the laser beam from the field of view of the receiver. Since the detection of slopes also relies on this phenomenon, the values of slopes that would register as obstacles would rely on the final laser system configuration. A preliminary

system configuration discussed in the next section uses an intercept point 2 m in advance of the vehicle and an obstacle threshold of 0.5 m. These system parameters would result in positive slopes of 23° and negative slopes of 15° appearing as obstacles.

In the long range mode (10 m) much smaller slopes will appear as formations which are greater than maximum negotiable obstacles at the detection point. The discrimination of negotiable slopes from non-negotiable obstacles in this mode would be extremely difficult. The philosophy in this mode would be to slow the vehicle down at the detection of any possible obstacle and make further observations at closer range.

Laser System Configuration - As a result of studies of laser systems the approach which appears to offer the most promise is that which uses a narrow beam laser and a limited field of view receiver and operates on the loss of return by interruption of beam path principle.

A typical configuration would mount a laser and scanner on the mast at approximately 2.5 m high with the receiver mounted 0.5 m below it for the slow mode. The beam would make a 64° angle with the mast. A well collimated laser beam could be scanned by either of the methods discussed previously. With this sensor configuration on a mast located 2.0 m back from the wheel front, the ground intercept point of the beam will be 2 m in front of the vehicle. Positive obstacles over 0.5 m and holes wider than 0.8 m and deeper than 0.5 m would interrupt the beam. The geometry for the slow mode is illustrated in Figure 27.

In the case of high speed (manned) operation a ground intercept at 10 m is required. This would require an angle of 78° with the mast if the laser is mounted as above. The receiver would be positioned at 80° to the mast and have about a 1/2° field. The resulting obstacle resolution would be roughly a 0.25 m positive obstacle and a 0.80-m-wide hole (deeper than 0.25 m).

The exact angles, detection points, obstacle sizes, etc. will depend on the eventual design and capabilities of the LRV.

The degree of scanning required will depend on the speed of the vehicle and the desired lateral coverage. Assuming a 3-m-wide vehicle traveling in a straight line, the sensor must scan  $\pm 8.5^\circ$  in the fast mode and  $\pm 20^\circ$  in the slow mode to cover the vehicle path. To account for turning a larger scan is needed. A sensor scan of  $\pm 30^\circ$  in both modes would provide additional lateral coverage of 0.8 m on either side

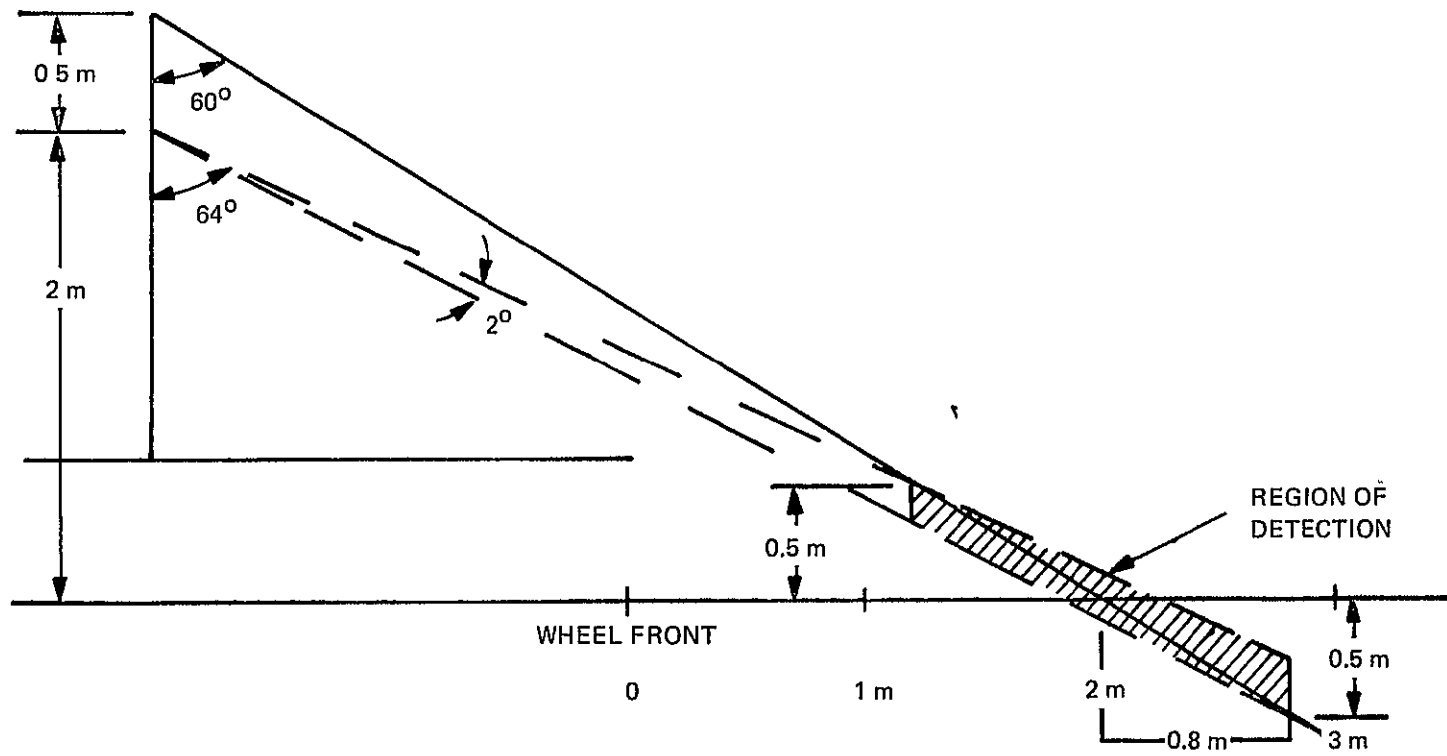


Figure 27 Laser Cane Geometry for Slow Mode

of the vehicle path in the slow mode and 5 m on either side of the vehicle path in the fast mode. Since the turns would be gentler in the slow mode than in the fast mode, less lateral coverage for turns would be required. These cases are illustrated in Figure 28.

The laser will be pulsed and both the pulse rate and scan rate must be selected. At 10 km/hr the vehicle covers a distance of 3 m in 1 sec. If the gap in forward coverage is to be limited to 30 cm there must be 10 scans/sec or a scan rate of 5 cps as a minimum. With 10 scans/sec and a laser pulsing at 1000 cps there will be 100 shots/scan. In the maximum lateral coverage case, a 30° scan at 10 m in front of the vehicle provides a 13-m-wide path. Thus one pulse would hit about every 13 cm and any obstacles to the LRV would be detected.

A simplified block diagram of a laser cane is shown in Figure 29. The pulser powers the Ga As laser and provides the clock rate for the scan driver and the logic. The laser beam is collimated and then the terrain is scanned. In this example the receiver consists of a linear array of photodiodes, each covering part of the field. These photodiodes feed into preamps (high gain video preamplifiers) and then into the logic. The logic basically is used to discern when a pulse has been lost and thus when an obstacle is present. By locating which detector was missed the location of obstacle is obtained. This would presumably be done by simple gates clocked by the pulser.

In summary, the laser cane system will meet the operational requirements for hazard detection equipment on the LRV. By adjusting the location and size of the area of target detection, the range and resolution required for either mode of operation will be obtainable. Comparison with laser systems of similar or greater complexity yields the following space, weight and power estimates: volume less than 1 ft<sup>3</sup>, weight less than 10 lb and power between 5 and 8 W average.

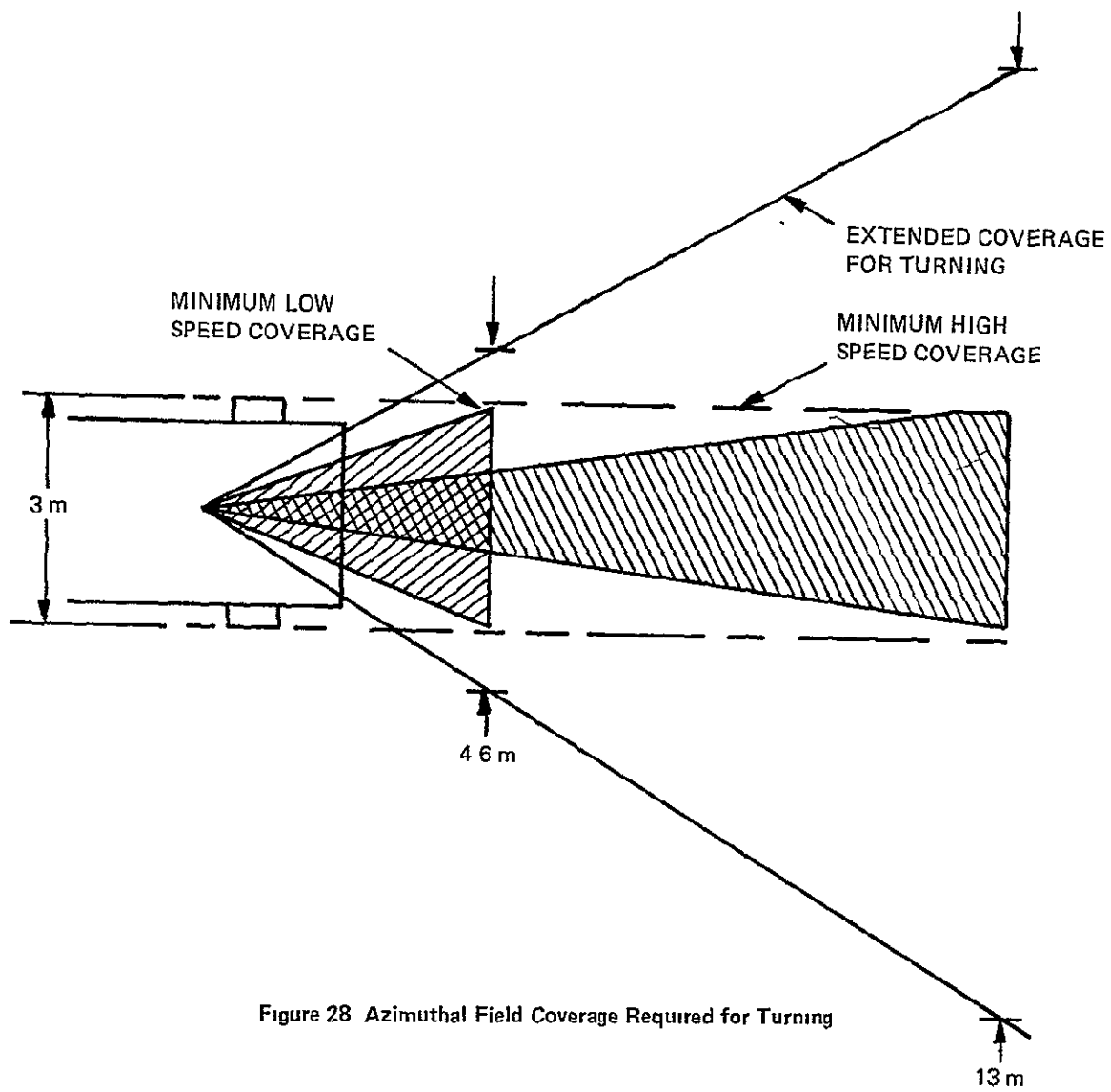


Figure 28 Azimuthal Field Coverage Required for Turning

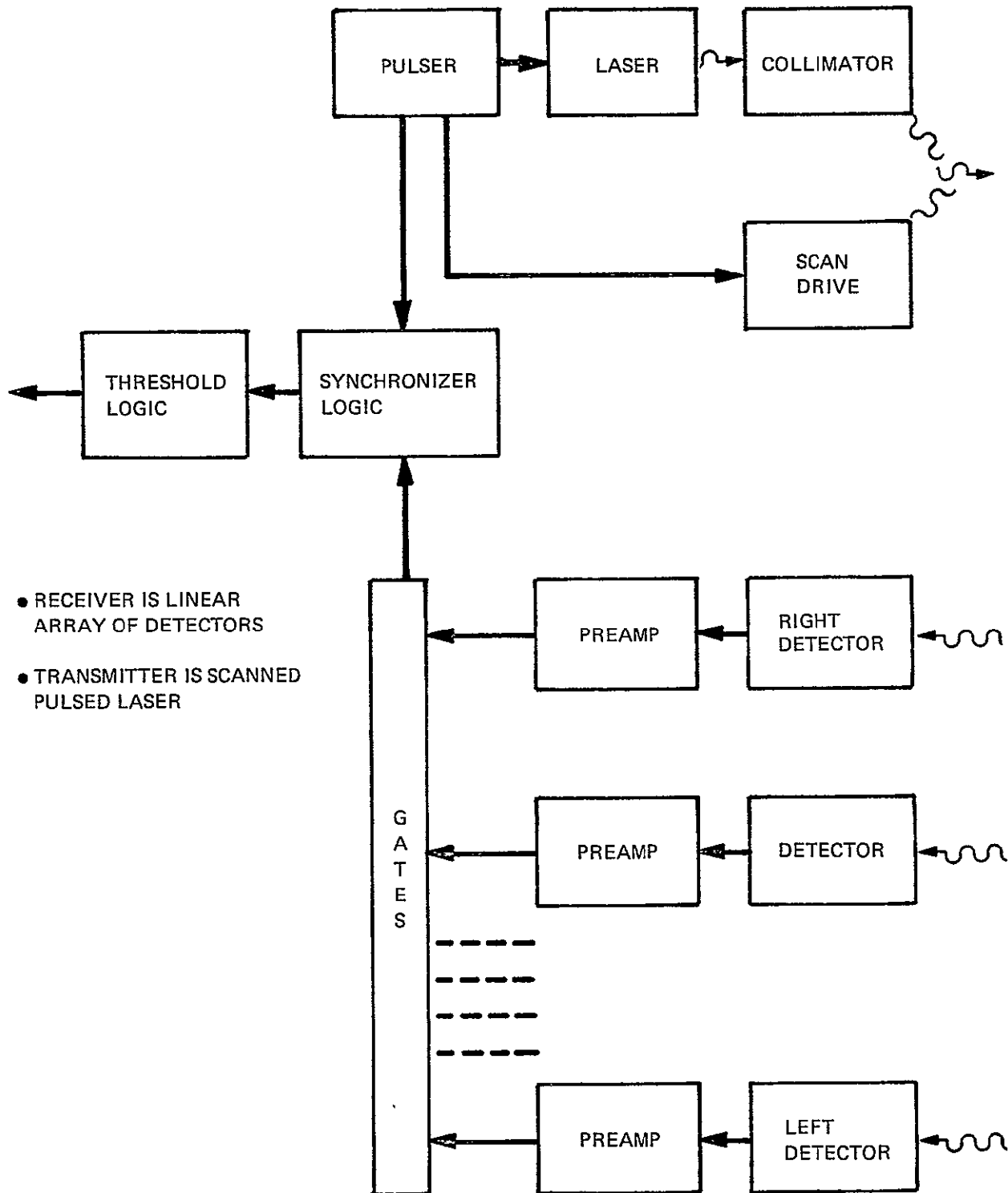


Figure 29 Laser Cane Simplified Block Diagram

